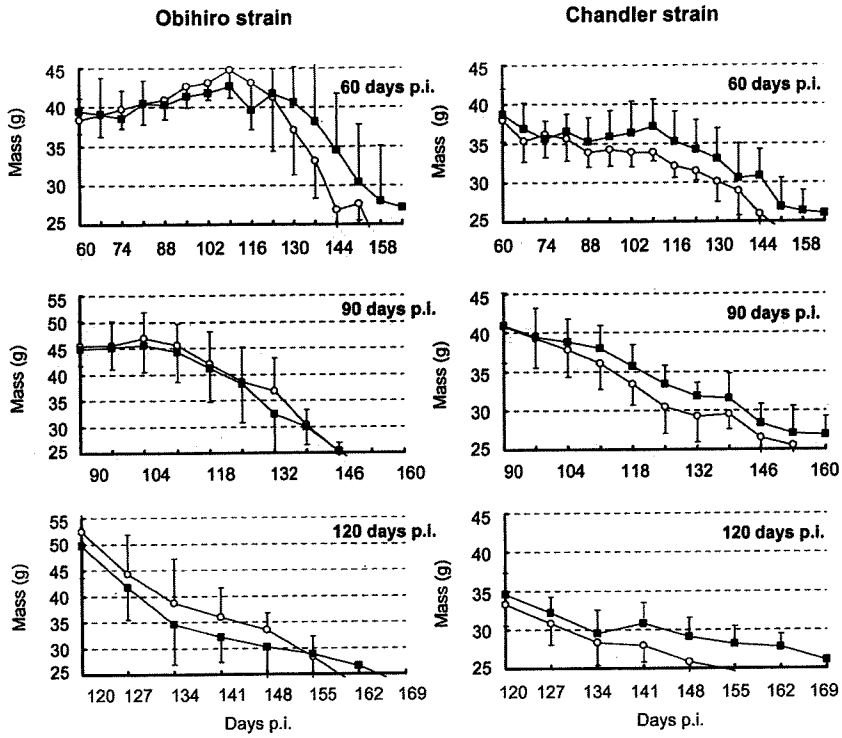


**Fig. 6.** Changes in body weight. After the initiation of mAb infusion, mice were weighed weekly up to the terminal stage of the disease. The groups of mice used in Fig. 5 were used to monitor body weight. ○, Mice treated with mAb P2-284; ■, mice treated with mAb 31C6.

to be milder than those observed in mice infused with the negative-control mAb. In contrast, no apparent reduction in microglial activation or astrogliosis by anti-PrP mAb was observed in the lateral cortex, where delivery of mAbs appeared to be inefficient (data not shown). It has been reported that the process of conversion of $PrP^{C}$ to $PrP^{Sc}$ on neurons rather than extracellular deposition of $PrP^{Sc}$ is involved in neuronal degeneration (Brandner *et al.*, 1996; Mallucci *et al.*, 2003; Chesebro *et al.*, 2005). Although the mechanism by which $PrP^{Sc}$ formation provokes microglial activation and astrogliosis remains to be elucidated, these results imply that arresting conversion of $PrP^{C}$ to $PrP^{Sc}$ via mAb infusion may contribute, at least to some extent, to the observed reduction in microglial activation and astrogliosis.

Previous results have shown that passive immunization with anti-PrP mAb via intraperitoneal injection does not have a protective effect after invasion of prion into the CNS or inoculation of prion via the intracerebral route (White *et al.*, 2003). In contrast, intraventricular infusion of anti-PrP mAb prolonged survival when mAb was infused at the time that $PrP^{Sc}$ became detectable in the CNS (e.g. at 60 days p.i.). The difference seems to be explained by inadequate transfer of anti-PrP mAbs into the CNS across the blood–brain barrier when mAbs are administered peripherally. Several compounds, including amphotericin B, PPS, porphyrin derivatives and GN8, have been reported to prolong the survival of mice infected with prion when administered at the middle or late stage of infection, but the animals were still prior to clinical onset (Demaimay *et al.*, 1997; Doh-ura *et al.*, 2004; Kocisko *et al.*, 2006; Kuwata *et al.*, 2007). To the best of our knowledge, there has been only one report of a treatment that prolongs survival of animals already in the clinical phase. Specifically, intraperitoneal administration of MS-8209 was shown to prolong survival of mice infected with the C506M3 strain when treatment was carried out at the time of the appearance of neurological symptoms (Demaimay *et al.*, 1997). Human prion diseases are usually detected after clinical onset and thus the availability of treatments that are effective even after symptoms have begun to appear is highly important. Therefore, it is of interest that intraventricular infusion of anti-PrP mAb was effective for prolongation of survival, even when treatment was initiated after the appearance of early clinical signs (at 120 days p.i.) in mice infected with the Chandler strain. Although in this study mAb infusion for 14 days of duration achieved only 8 % prolongation, the result should encourage further trials with mAbs that may be useful in the development of therapeutic treatment for prion diseases. For instance, continuing treatment over a longer duration, which may keep the effective concentration of mAbs in the brain higher over a longer period of time, may improve the effect on survival. In addition, anti-PrP mAb prolonged survival, despite the fact that the infused mAb was not evenly distributed in the brain but rather was primarily restricted to the hippocampus and thalamus. Thus, it is conceivable that improved delivery of mAb might enhance the effects of anti-PrP mAb on survival. Fab and single-chain antibody fragments have also been shown to inhibit $PrP^{Sc}$ formation (Peretz *et al.*, 2001; Donofrio *et al.*, 2005), and the smaller size of these fragments may be beneficial for efficient delivery in tissues.

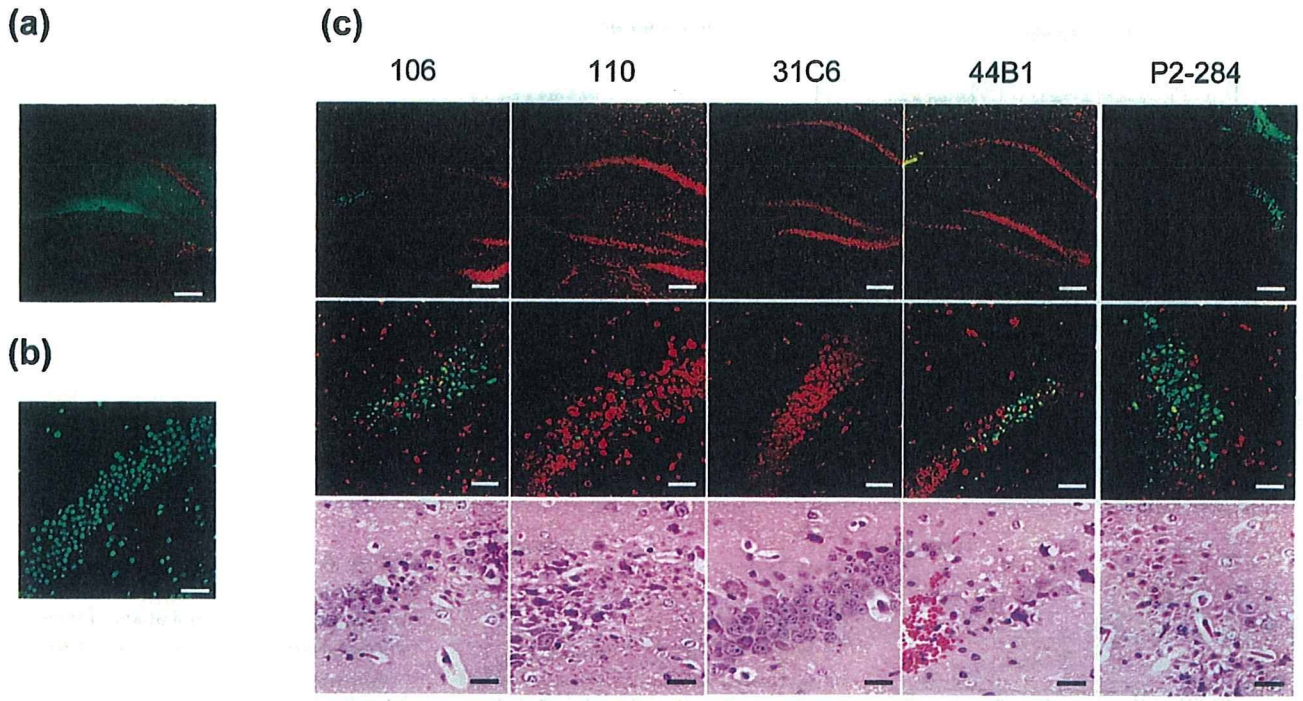


**Fig. 7.** Neuronal toxicity of anti-PrP mAbs. Anti-PrP mAbs (106, 110, 31C6 or 44B1) and the negative-control mAb P2-284 were injected into the left and right hippocampus, respectively, using stereotaxic apparatus. Seventy-two hours after injection, brains were obtained and fixed in 10 % formalin. Paraffin sections were subjected to TUNEL and H&E staining. (a) Distribution of mAb. Alexa Fluor 488-conjugated mAb 31C6 was injected into the hippocampus and the distribution was analysed by confocal laser microscopy. (b) Positive control. Coronal sections were pre-treated with DNase I and then stained using the TUNEL procedure. The pyramidal cell layers of the hippocampus are shown. (c) TUNEL- and H&E-stained samples. Low-magnification (top panels) and high-magnification micrographs (middle panels) of TUNEL-stained samples and corresponding H&E-stained samples (bottom panels) are shown. The mAbs injected are indicated above the panels. Three to six mice were examined for each mAb. Bars, 200 μm.

Although mice infected with either the Obihiro or Chandler strain succumbed to the disease at around 150 days p.i., the effect of mAb infusion on survival differed when administered to mice challenged with different prion strains. For example, mAb infusion of mice infected with the Chandler strain was effective when the mAb was administered at any of the three time points tested (60, 90 and 120 days p.i.), whereas no prolongation was observed in mice infected with the Obihiro strain when mAb infusion was initiated at 90 or 120 days p.i. (Fig. 6). At present, we do not have a precise explanation for this but can speculate on what might explain the difference. First, microglial activation in mice infected with the Obihiro strain was more severe than that in mice infected with the Chandler strain (Figs 3 and 4). Similar to the mouse model for Alzheimer's disease (El Khoury *et al.*, 2007), microglial recruitment is expected to have a protective role in prion disease; however, activated microglia also have neurotoxic effects via production of cytokines, chemokines and reactive oxygen species (Bate *et al.*, 2001, 2002; Marella *et al.*, 2005). Thus, even when mitigated by anti-PrP mAb, the severe microglial activation in mice infected with Obihiro strain may be sufficient for progression of the disease. Secondly, differences in the distribution of $PrP^{Sc}$ may account for the differences in the effect of anti-PrP mAb in one prion strain versus the other. For instance, $PrP^{Sc}$ accumulation in the hypothalamus of mice infected with the Obihiro strain was more severe than that in mice infected with the Chandler strain (data not shown). Moreover, $PrP^{Sc}$ formation in the hypothalamus might not be inhibited efficiently due to the uneven distribution of mAb in the hypothalamus (Fig. 1). These results may explain in part the lack of prolongation in the Obihiro strain-infected mice infused with mAb at 90 or 120 days p.i.

Immunotherapy has been of interest in the treatment of Alzheimer's disease; however, the fact that immunization of β-amyloid peptide caused meningoencephalitis in some patients in clinical trials warns of the adverse effects of autoimmune reactions *in vivo* (Check, 2002; Nicoll *et al.*, 2003; Orgogozo *et al.*, 2003). Additionally, cross-linking of $PrP^{C}$ by an anti-PrP mAb that recognizes a specific epitope (aa 95–105) provoked degeneration of hippocampal and cerebellar neurons (Solforosi *et al.*, 2004). These adverse effects of antibodies on the CNS have prompted extreme

caution in the use of anti-PrP antibodies, in particular, their introduction into the CNS. However, passive immunization is less likely to initiate an autoimmune reaction (Schenk, 2002; Sadowski & Wisniewski, 2004). In this study, we observed no antibody-induced inflammation by intraventricular infusion. In addition, neuronal death in the hippocampus was not observed, even though mAbs 106 and 110, which recognize the region adjacent to aa 95–105, were injected directly into the hippocampus. Although the potential adverse effects, especially an inflammatory response, should be examined carefully, the fact that anti-PrP mAbs interfered with disease progression, even when administered after clinical onset, is particularly encouraging. Although the effect of anti-PrP mAb differed in prion strains, this implies that the immunotherapy might be effective in certain types of human prion disease, if not all. Therefore, the results of this study should promote further efforts to improve the effect of anti-PrP mAbs, such as the form of the antibody, the route of administration and an efficient way of delivering the antibodies.

## ACKNOWLEDGEMENTS

This work was supported by the Regional New Consortium R&D Projects from the Ministry of Economy, Trade and Industry, a grant from The 21st Century COE Program (A-1) and a Grant-in-Aid for Science Research (A) (grant no. 18208026) from the Ministry of Education, Culture, Sports, Science and Technology of Japan. This work was also supported by a grant from the Ministry of Health, Labour and Welfare of Japan (grant no. 17270701). This work was also partly supported by a grant for Strategic Cooperation to Control Emerging and Re-emerging Infections and the Program of Founding Research Centers for Emerging and Reemerging Infectious Diseases, from the Ministry of Education, Culture, Sports, Science and Technology, Japan.

## REFERENCES

**Bate, C., Reid, S. & Williams, A. (2001).** Killing of prion-damaged neurones by microglia. *Neuroreport* **12**, 2589–2594.

**Bate, C., Boshuizen, R. S., Langeveld, J. P. & Williams, A. (2002).** Temporal and spatial relationship between the death of PrP-damaged neurones and microglial activation. *Neuroreport* **13**, 1695–1700.

**Brandner, S., Isenmann, S., Raeber, A., Fischer, M., Sailer, A., Kobayashi, Y., Marino, S., Weissmann, C. & Aguzzi, A. (1996).** Normal host prion protein necessary for scrapie-induced neurotoxicity. *Nature* **379**, 339–343.

**Check, E. (2002).** Nerve inflammation halts trial for Alzheimer's drug. *Nature* **415**, 462.

**Chesebro, B., Race, R. & Kercher, L. (2005).** Scrapie pathogenesis in brain and retina: effects of prion protein expression in neurons and astrocytes. *J Neurovirol* **11**, 476–480.

**Demaimay, R., Adjou, K. T., Beringue, V., Demart, S., Lasmézas, C. I., Deslys, J. P., Seman, M. & Dormont, D. (1997).** Late treatment with polyene antibiotics can prolong the survival time of scrapie-infected animals. *J Virol* **71**, 9685–9689.

**Doh-ura, K., Ishikawa, K., Murakami-Kubo, I., Sasaki, K., Mohri, S., Race, R. & Iwaki, T. (2004).** Treatment of transmissible spongiform encephalopathy by intraventricular drug infusion in animal models. *J Virol* **78**, 4999–5006.

**Donofrio, G., Heppner, F. L., Polymenidou, M., Musahl, C. & Aguzzi, A. (2005).** Paracrine inhibition of prion propagation by anti-PrP single-chain Fv miniantibodies. *J Virol* **79**, 8330–8338.

**Ehlers, B. & Diringer, H. (1984).** Dextran sulphate 500 delays and prevents mouse scrapie by impairment of agent replication in spleen. *J Gen Virol* **65**, 1325–1330.

**El Khoury, J., Toft, M., Hickman, S. E., Means, T. K., Terada, K., Geula, C. & Luster, A. D. (2007).** Ccr2 deficiency impairs microglial accumulation and accelerates progression of Alzheimer-like disease. *Nat Med* **13**, 432–438.

**Enari, M., Flechsig, E. & Weissmann, C. (2001).** Scrapie prion protein accumulation by scrapie-infected neuroblastoma cells abrogated by exposure to a prion protein antibody. *Proc Natl Acad Sci U S A* **98**, 9295–9299.

**Farquhar, C. F. & Dickinson, A. G. (1986).** Prolongation of scrapie incubation period by an injection of dextran sulphate 500 within the month before or after infection. *J Gen Virol* **67**, 463–473.

**Feraudet, C., Morel, N., Simon, S., Volland, H., Frobert, Y., Creminon, C., Vilette, D., Lehmann, S. & Grassi, J. (2005).** Screening of 145 anti-PrP monoclonal antibodies for their capacity to inhibit $PrP^{Sc}$ replication in infected cells. *J Biol Chem* **280**, 11247–11258.

**Fernandez-Borges, N., Brun, A., Whitton, J. L., Parra, B., Diaz-San Segundo, F., Salguero, F. J., Torres, J. M. & Rodriguez, F. (2006).** DNA vaccination can break immunological tolerance to PrP in wild-type mice and attenuates prion disease after intracerebral challenge. *J Virol* **80**, 9970–9976.

**Furuoka, H., Yabuzoe, A., Horiuchi, M., Tagawa, Y., Yokoyama, T., Yamakawa, Y., Shinagawa, M. & Sata, T. (2005).** Effective antigen-retrieval method for immunohistochemical detection of abnormal isoform of prion proteins in animals. *Acta Neuropathol* **109**, 263–271.

**Gilch, S., Wopfner, F., Renner-Muller, I., Kremmer, E., Bauer, C., Wolf, E., Brem, G., Groschup, M. H. & Schatzl, H. M. (2003).** Polyclonal anti-PrP auto-antibodies induced with dimeric PrP interfere efficiently with $PrP^{Sc}$ propagation in prion-infected cells. *J Biol Chem* **278**, 18524–18531.

**Goñi, F., Knudsen, E., Schreiber, F., Scholtzova, H., Pankiewicz, J., Carp, R., Meeker, H. C., Rubenstein, R., Brown, D. R. & other authors (2005).** Mucosal vaccination delays or prevents prion infection via an oral route. *Neuroscience* **133**, 413–421.

**Heppner, F. L., Musahl, C., Arrighi, I., Klein, M. A., Rülicke, T., Oesch, B., Zinkernagel, R. M., Kalinke, U. & Aguzzi, A. (2001).** Prevention of scrapie pathogenesis by transgenic expression of anti-prion protein antibodies. *Science* **294**, 178–182.

**Horiuchi, M. & Caughey, B. (1999).** Specific binding of normal prion protein to the scrapie form via a localized domain initiates its conversion to the protease-resistant state. *EMBO J* **18**, 3193–3203.

**Horiuchi, M., Yamazaki, N., Ikeda, T., Ishiguro, N. & Shinagawa, M. (1995).** A cellular form of prion protein ($PrP^{C}$) exists in many non-neuronal tissues of sheep. *J Gen Virol* **76**, 2583–2587.

**Horiuchi, M., Mochizuki, M., Ishiguro, N., Nagasawa, H. & Shinagawa, M. (1997).** Epitope mapping of a monoclonal antibody specific to feline panleukopenia virus and mink enteritis virus. *J Vet Med Sci* **59**, 133–136.

**Kaneko, K., Peretz, D., Pan, K. M., Blochberger, T. C., Wille, H., Gabizon, R., Griffith, O. H., Cohen, F. E., Baldwin, M. A. & Prusiner, S. B. (1995).** Prion protein (PrP) synthetic peptides induce cellular PrP to acquire properties of the scrapie isoform. *Proc Natl Acad Sci U S A* **92**, 11160–11164.

**Kim, C. L., Umetani, A., Matsui, T., Ishiguro, N., Shinagawa, M. & Horiuchi, M. (2004a).** Antigenic characterization of an abnormal

isoform of prion protein using a new diverse panel of monoclonal antibodies. *Virology* **320**, 40–51.

**Kim, C. L., Karino, A., Ishiguro, N., Shinagawa, M., Sato, M. & Horiuchi, M. (2004b).** Cell-surface retention of $PrP^C$ by anti-PrP antibody prevents protease-resistant PrP formation. *J Gen Virol* **85**, 3473–3482.

**Kocisko, D. A., Caughey, W. S., Race, R. E., Roper, G., Caughey, B. & Morrey, J. D. (2006).** A porphyrin increases survival time of mice after intracerebral prion infection. *Antimicrob Agents Chemother* **50**, 759–761.

**Kuwata, K., Nishida, N., Matsumoto, T., Kamatari, Y. O., Hosokawa-Muto, J., Kodama, K., Nakamura, H. K., Kimura, K., Kawasaki, M. & other authors (2007).** Hot spots in prion protein for pathogenic conversion. *Proc Natl Acad Sci U S A* **104**, 11921–11926.

**Ladogana, A., Casaccia, P., Ingrosso, L., Cibati, M., Salvatore, M., Xi, Y. G., Masullo, C. & Pocchiari, M. (1992).** Sulphate polyanions prolong the incubation period of scrapie-infected hamsters. *J Gen Virol* **73**, 661–665.

**Mallucci, G., Dickinson, A., Linehan, J., Klöhn, P. C., Brandner, S. & Collinge, J. (2003).** Depleting neuronal PrP in prion infection prevents disease and reverses spongiosis. *Science* **302**, 871–874.

**Marella, M., Gaggioli, C., Batoz, M., Deckert, M., Tartare-Deckert, S. & Chabry, J. (2005).** Pathological prion protein exposure switches on neuronal mitogen-activated protein kinase pathway resulting in microglia recruitment. *J Biol Chem* **280**, 1529–1534.

**Morrissey, M. P. & Shakhnovich, E. I. (1999).** Evidence for the role of $PrP^C$ helix 1 in the hydrophilic seeding of prion aggregates. *Proc Natl Acad Sci U S A* **96**, 11293–11298.

**Nicoll, J. A., Wilkinson, D., Holmes, C., Steart, P., Markham, H. & Weller, R. O. (2003).** Neuropathology of human Alzheimer disease after immunization with amyloid-$\beta$ peptide: a case report. *Nat Med* **9**, 448–452.

**Orgogozo, J. M., Gilman, S., Dartigues, J. F., Laurent, B., Puel, M., Kirby, L. C., Jouanny, P., Dubois, B., Eisner, L. & other authors (2003).** Subacute meningoencephalitis in a subset of patients with AD after A$\beta$42 immunization. *Neurology* **61**, 46–54.

**Paxinos, G. & Franklin, K. B. J. (2001).** *The Mouse Brain in Stereotaxic Coordinates*, 2nd edn. San Diego: Academic Press.

**Peretz, D., Williamson, R. A., Kaneko, K., Vergara, J., Leclerc, E., Schmitt-Ulm, G., Mehlhorn, I. R., Legname, G., Wormald, M. R. & other authors (2001).** Antibodies inhibit prion propagation and clear cell cultures of prion infectivity. *Nature* **412**, 739–743.

**Perrier, V., Solassol, J., Crozet, C., Frobert, Y., Mourton-Gilles, C., Grassi, J. & Lehmann, S. (2004).** Anti-PrP antibodies block $PrP^{Sc}$ replication in prion-infected cell cultures by accelerating $PrP^C$ degradation. *J Neurochem* **89**, 454–463.

**Priola, S. A., Raines, A. & Caughey, W. S. (2000).** Porphyrin and phthalocyanine antiscrapie compounds. *Science* **287**, 1503–1506.

**Rainov, N. G., Tsuboi, Y., Krolak-Salmon, P., Vighetto, A. & Doh-Ura, K. (2007).** Experimental treatments for human transmissible spongiform encephalopathies: is there a role for pentosan polysulfate? *Expert Opin Biol Ther* **7**, 713–726.

**Sadowski, M. & Wisniewski, T. (2004).** Vaccines for conformational disorders. *Expert Rev Vaccines* **3**, 279–290.

**Schenk, D. (2002).** Amyloid-$\beta$ immunotherapy for Alzheimer's disease: the end of the beginning. *Nat Rev Neurosci* **3**, 824–828.

**Schwarz, A., Krätke, O., Burwinkel, M., Riemer, C., Schultz, J., Henklein, P., Bamme, T. & Baier, M. (2003).** Immunisation with a synthetic prion protein-derived peptide prolongs survival times of mice orally exposed to the scrapie agent. *Neurosci Lett* **350**, 187–189.

**Sigurdsson, E. M., Brown, D. R., Daniels, M., Kascsak, R. J., Kascsak, R., Carp, R., Meeker, H. C., Frangione, B. & Wisniewski, T. (2002).** Immunization delays the onset of prion disease in mice. *Am J Pathol* **161**, 13–17.

**Solforosi, L., Criado, J. R., McGavern, D. B., Wirz, S., Sánchez-Alavez, M., Sugama, S., DeGiorgio, L. A., Volpe, B. T., Wiseman, E. & other authors (2004).** Cross-linking cellular prion protein triggers neuronal apoptosis in vivo. *Science* **303**, 1514–1516.

**Speare, J. O., Rush, T. S., III, Bloom, M. E. & Caughey, B. (2003).** The role of helix 1 aspartates and salt bridges in the stability and conversion of prion protein. *J Biol Chem* **278**, 12522–12529.

**Todd, N. V., Morrow, J., Doh-ura, K., Dealler, S., O'Hare, S., Farling, P., Duddy, M. & Rainov, N. G. (2005).** Cerebroventricular infusion of pentosan polysulphate in human variant Creutzfeldt–Jakob disease. *J Infect* **50**, 394–396.

**Trevitt, C. R. & Collinge, J. (2006).** A systematic review of prion therapeutics in experimental models. *Brain* **129**, 2241–2265.

**Uryu, M., Karino, A., Kamihara, Y. & Horiuchi, M. (2007).** Characterization of prion susceptibility in Neuro2a mouse neuroblastoma cell subclones. *Microbiol Immunol* **51**, 661–667.

**White, A. R., Enever, P., Tayebi, M., Mushens, R., Linehan, J., Brandner, S., Anstee, D., Collinge, J. & Hawke, S. (2003).** Monoclonal antibodies inhibit prion replication and delay the development of prion disease. *Nature* **422**, 80–83.

Microbiol. Immunol., 51(7), 661–669, 2007

# Characterization of Prion Susceptibility in Neuro2a Mouse Neuroblastoma Cell Subclones

**Masahide Uryu[1], Ayako Karino[2], Yukiko Kamihara[1], and Motohiro Horiuchi*[,1]**

[1]*Laboratory of Prion Diseases, Graduate School of Veterinary Medicine, Hokkaido University, Sapporo, Hokkaido 060–0818, Japan, and* [2]*Department of Veterinary Public Health, Obihiro University of Agriculture and Veterinary Medicine, Obihiro, Hokkaido 080–8555, Japan*

Received January 31, 2007; in revised form, April 26, 2007. Accepted May 21, 2007

***Abstract*: In this study, we established Neuro2a (N2a) neuroblastoma subclones and characterized their susceptibility to prion infection. The N2a cells were treated with brain homogenates from mice infected with mouse prion strain Chandler. Of 31 N2a subclones, 19 were susceptible to prion as those cells became positive for abnormal isoform of prion protein ($PrP^{Sc}$) for up to 9 serial passages, and the remaining 12 subclones were classified as unsusceptible. The susceptible N2a subclones expressed cellular prion protein ($PrP^{C}$) at levels similar to the parental N2a cells. In contrast, there was a variation in $PrP^{C}$ expression in unsusceptible N2a subclones. For example, subclone N2a-1 expressed $PrP^{C}$ at the same level as the parental N2a cells and prion-susceptible subclones, whereas subclone N2a-24 expressed much lower levels of PrP mRNA and $PrP^{C}$ than the parental N2a cells. There was no difference in the binding of $PrP^{Sc}$ to prion-susceptible and unsusceptible N2a subclones regardless of their $PrP^{C}$ expression level, suggesting that the binding of $PrP^{Sc}$ to cells is not a major determinant for prion susceptibility. Stable expression of $PrP^{C}$ did not confer susceptibility to prion in unsusceptible subclones. Furthermore, the existence of prion-unsusceptible N2a subclones that expressed $PrP^{C}$ at levels similar to prion-susceptible subclones, indicated that a host factor(s) other than $PrP^{C}$ and/or specific cellular microenvironments are required for the propagation of prion in N2a cells. The prion-susceptible and -unsusceptible N2a subclones established in this study should be useful for identifying the host factor(s) involved in the prion propagation.**

*Key words*: **Neuro2a, Prion, PrP, Susceptibility**

Transmissible spongiform encephalopathies, so-called prion diseases, are fatal neurodegenerative disorders that include scrapie in sheep and goats, bovine spongiform encephalopathy, and Creutzfeldt-Jakob disease in humans. The major component of causative agent of prion diseases, prion, is thought to be an abnormal isoform of prion protein ($PrP^{Sc}$). $PrP^{Sc}$ is generated from a normal cellular prion protein ($PrP^{C}$) by certain post-translational modifications and the process in the conversion of $PrP^{C}$ to $PrP^{Sc}$ is considered to be a central event in pathogenesis of prion diseases (31). $PrP^{C}$ is a sialo-glycoprotein expressed on the cell surface as a glycosyl-phosphatidylinositol anchoring protein (36). Cell biological studies have revealed that mature $PrP^{C}$ on the cell surface acts as a substrate for the $PrP^{Sc}$ biosynthesis, and formation of $PrP^{Sc}$ takes place either at the cell membrane or during the endocytic pathway (3, 8, 37). Depletion of cholesterol inhibits $PrP^{Sc}$ formation in prion-infected cells (2, 38), and the co-existence of $PrP^{C}$ and $PrP^{Sc}$ in lipid rafts or caveolae-like domains suggests that cholesterol- and sphingolipid-enriched membrane microdomains are sites for the interaction between $PrP^{C}$ and $PrP^{Sc}$ (29, 41).

Although $PrP^{C}$ is essential for the propagation of prion and the development of prion diseases (6), other host factors are thought to be involved in the $PrP^{Sc}$ formation, i.e., prion replication. Studies using chimeric

**Address correspondence to* Dr. Motohiro Horiuchi, Laboratory of Prion Diseases, Graduate School of Veterinary Medicine, Hokkaido University, Kita 18, Nishi 9, Kita-ku, Sapporo, Hokkaido 060–0818, Japan. Fax: +81–11–706–5293. E-mail: horiuchi@vetmed.hokudai.ac.jp

*Abbreviations*: CHO, Chinese hamster ovary; DMEM, Dulbecco's modified Eagle's medium; FBS, fetal bovine serum; GAPDH, glyceraldehyde-3-phosphate dehydrogenase; HS, heparan sulfate; LRP/LR, laminin receptor precursor/laminin receptor; MAb, monoclonal antibody; N2a, Neuro2a; PBS, phosphate-buffered saline; PrP, prion protein; $PrP^{C}$, cellular prion protein; $PrP^{Sc}$, abnormal isoform of prion protein; RT-PCR, reverse transcription-polymerase chain reaction; SDS-PAGE, sodium dodecyl sulfate-polyacrylamide gel electrophoresis; WB, Western blotting.

and point mutants of PrP have suggested that a host factor designated Protein X is required for prion propagation (18, 40), although its identity remains unknown. To date, Bcl-2 (21), laminin receptor precursor/laminin receptor (LRP/LR) (32), neural cell adhesion molecule (35), and several other proteins have been identified as possible counterparts of $PrP^{C}$. Plasminogen has been reported to bind $PrP^{Sc}$ (11). In addition, a reduction in the level of LRP/LR inhibits $PrP^{Sc}$ formation in prion-infected cells, suggesting that the LRP/LR has a direct or indirect role in prion propagation (22). The biological significance of other proteins in prion propagation remains unclear (34, 35).

Recently, cysteine proteases, such as calpain, and cathepsin B and L were reported to modulate $PrP^{Sc}$ formation (23, 42). Furthermore, inhibitors of c-Abl tyrosine kinase and mitogen-activated protein kinase kinase are reported to accelerate $PrP^{Sc}$ degradation in prion-infected cells (10, 30). Thus, changes in the cellular microenvironment, by interfering with cellular signaling, may also affect prion propagation. These findings suggest the involvement of other host factors for prion propagation. Identification of such host factors and cellular microenvironments involved in prion propagation is of great interest not only for understanding the basic mechanisms of prion propagation but also for finding new therapeutic targets.

Comparative analyses between permissive and non-permissive conditions for prion propagation will facilitate the identification of the host factors involved in prion propagation. In the present study, we established subclones of mouse Neuro2a (N2a) neuroblastoma cells and analyzed their susceptibility to prion. The prion-susceptible and -unsusceptible subclones established in this study should be useful for identifying host factors involved in prion replication.

## Materials and Methods

*Cell culture and cloning of the cells.* N2a cell line (American Type Culture Collection CCL-131, 58th passage at the purchase) was grown in Dulbecco's modified Eagle's medium with high glucose (DMEM; ICN Biomedicals), 10% fetal bovine serum (FBS), and non-essential amino acids. N2a subclones were obtained by limiting dilution.

*Inoculation of prion to N2a cells.* Mouse prion strain Chandler was propagated in ICR mice (CLEA Japan, Inc.). The brains of mice at the terminal stage of the disease were homogenized in phosphate-buffered saline (PBS) at 10% (w/w) and the homogenates were stored at −30 C until use. The brain homogenate was diluted to 2% with the medium, and 500 μl was added to N2a cells in 60-mm dishes containing 1 ml of medium. After 24 hr, the medium was refreshed, and cells were serially passaged every 3 to 4 days at a 1:10 dilution.

*Detection of $PrP^{Sc}$.* Preparation and detection of $PrP^{Sc}$ in the prion-infected cells were carried out as described previously (19, 20) with slight modifications. Cells were lysed in lysis buffer (0.5% Triton X-100, 0.5% sodium deoxycholate, 10 mM Tris-HCl, pH 7.5, 150 mM NaCl, and 5 mM EDTA), and small aliquots of the lysates were stored for the determination of the protein concentration. The remaining lysates were digested with 20 μg/ml proteinase K at 37 C for 20 min. The digestion was stopped by the addition of Pefabloc (Roche) to 5 mM. The mixture was adjusted to 0.3% phosphotungstic acid by addition of a 5% solution and then incubated for 30 min at 37 C with constant rotation. $PrP^{Sc}$ was then collected by centrifugation at 20,000 × *g* for 20 min and subjected to SDS-PAGE followed by Western blotting (WB). Blots were probed with monoclonal antibody (mAb) 31C6 (20) and horseradish peroxidase-conjugated sheep $F(ab')_2$ fragment of anti-mouse IgG (Amersham Bioscience). The specific bands were visualized with ECL Western Blotting Detection Reagents (Amersham Bioscience) and a LAS-3000 chemiluminescence image analyzer (Fujifilm). Quantitative analyses of the blots were carried out with Image Reader LAS-3000 version 1.11 (Fujifilm).

*Flow cytometry.* Flow cytometric analysis was performed as described previously (19).

*$PrP^{Sc}$ binding assay.* Cells were seeded at $2.5 \times 10^4$ cells/well in 6-well plates and grown for 48 hr. Cells were then fed with 500 μl of the fresh medium and inoculated with 250 μl of 0.4 to 2% prion-infected mouse brain homogenate diluted with medium, and kept for 3 hr at either 37 C or on ice with occasional tilting. After the incubation, cells were washed with PBS three times, and bound $PrP^{Sc}$ was detected as described in detection of $PrP^{Sc}$.

*Quantitative reverse transcription-polymerase chain reaction (RT-PCR) analysis.* Total RNA was isolated from the cells with TRIzol Reagent (Invitrogen Life Technologies). First strand cDNA was synthesized from the total RNA using a First-Strand Synthesis Kit (Amersham Biosciences) according to the manufacturer's instructions. Real-time *Taq*Man PCR assays were performed to determine the relative quantity of mouse PrP gene expression. Amplification reaction mixtures contained template cDNA, 1X pre-designed set of primers and a *Taq*Man probe targeting the boundary between exons 1 and 2 of the PrP gene (*Taq*Man Gene Expression Assays No. Mm-00448389), and 1X *Taq*-

Man Universal PCR Master Mix (Applied Biosystems) in a final reaction volume of 20 μl. The amplification profile was monitored with an ABI PRISM 7900HT (Applied Biosystems), and the relative quantity was determined by the standard curve method (1) using SDS Plate Utility version 2.1 (Applied Biosystems). Expression of glyceraldehyde-3-phosphate dehydrogenase (GAPDH) gene was monitored as an endogenous control using *Taq*Man Rodent-GAPDH Control Reagents (Applied Biosystems).

*Cellular cholesterol content of N2a subclones.* Cells were seeded in 6-well plates in DMEM containing 10% FBS. After 48 hr, the medium was changed to Opti-MEM (Gibco) and cells were kept for additional 24 hr. Then, cells were washed three times with PBS and lysed with PBS containing 0.1% Triton X-100. The lysates were frozen at −30 C until use. The lysates were clarified by centrifugation at 20,000 × *g* for 15 min at 4 C, and the resulting supernatants were assayed for cholesterol using an Amplex Red Cholesterol Assay Kit (Molecular Probes) according to the manufacturer's instructions. Fluorescence was measured with a fluorescence microplate reader ARVO-SX (Wallac) using excitation at 560 nm and detection at 580 nm.

*Stable expression of $MoPrP^C$.* Eukaryotic expression vector, pRc/EF-MoPrP (M. H. and A. K. manuscript in preparation), which contains a mouse PrP cDNA expression unit driven by peptide chain elongation factor 1α promoter (27) along with the bacterial aminoglycoside phosphotransferase gene (G418 resistant gene) expression unit, was introduced into N2a cells with FuGENE 6 (Roche). The transfected cells were cultured in the presence of 0.3 mg/ml G418 (Gibco), and G418-resistant cells were selected. The cells were stained with anti-PrP mAb as described for the flow cytometric analysis (19), and cell sorting was performed using an EPICS ALTRA flow cytometer (Beckman Coulter). The cells with fluorescence intensities ranging from 100 to 500 were recovered and cultured with DMEM. Cells passaged more than 3 times were used for prion infection experiments.

## Results

*Prion-Susceptibility of N2a Subclones*

We isolated 31 N2a subclones by limiting dilution and examined them for susceptibility to prion. The N2a subclones were inoculated with scrapie Chandler strain-infected mouse brain homogenates, and prion-susceptibility was determined by the presence of $PrP^{Sc}$ during nine passages after inoculation. Figure 1 shows the representative results for $PrP^{Sc}$ detection in the N2a subclones at the third, sixth, and ninth passages after inoculation. Of 31 N2a subclones, 19 (N2a-2, -3, -5, -6, -7, -17, -21, -22, and -25 in Fig.1) were judged to be prion-susceptible, and the remaining 12 subclones (N2a-1, -4,

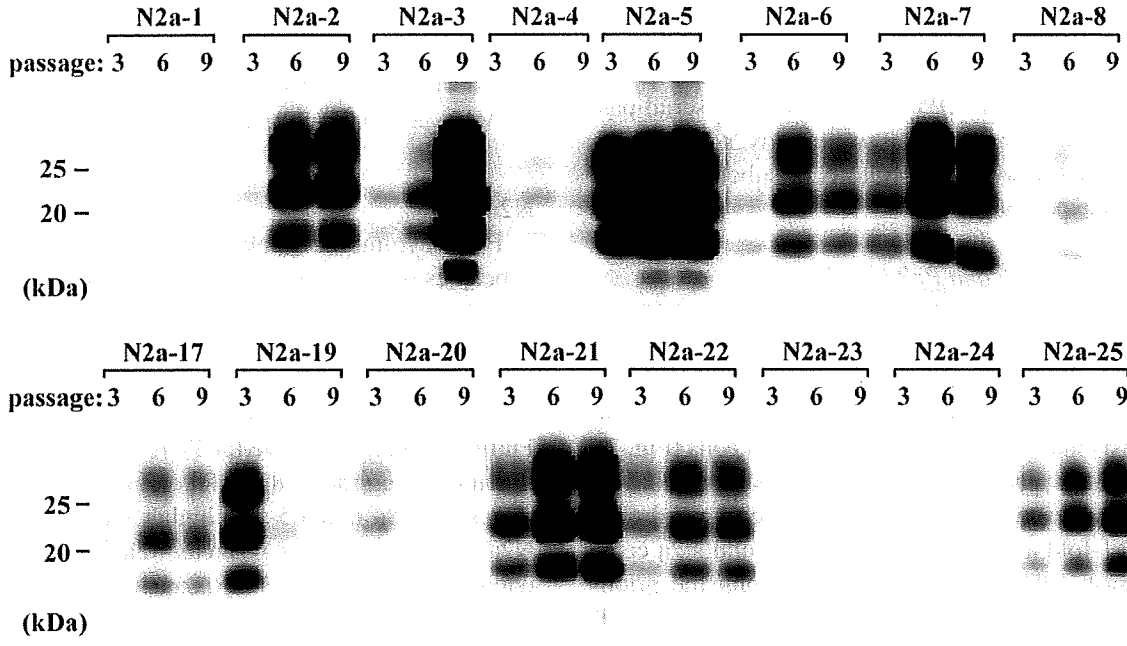


Fig. 1. Detection of $PrP^{Sc}$ in N2a subclones inoculated with prion. N2a subclones were inoculated with 2% brain homogenate from mice infected with Chandler strain, and then consecutively passaged up to nine times. The presence of $PrP^{Sc}$ was examined at the third, sixth, and ninth passages by WB. $PrP^{Sc}$-enriched sample derived from 0.1 mg of the cell lysates was loaded on each lane, and $PrP^{Sc}$ was detected with mAb 31C6. Results of representative N2a subclones are indicated. Molecular markers are indicated on the left.

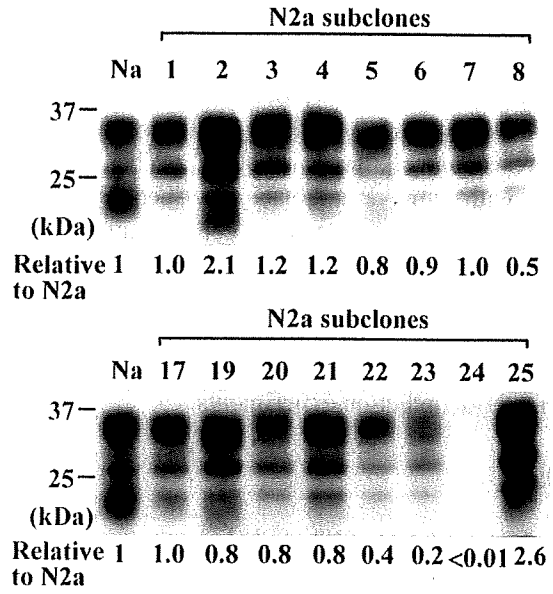


Fig. 2. Expression of $PrP^C$ in N2a subclones. Ten micrograms of cell lysates were loaded on each lane, and $PrP^C$ was detected with mAb 31C6. Na indicates parental N2a cells, and the numbers on the top of the images indicate the number of N2a subclones. Results of representative N2a subclones are indicated. The luminescence intensities were quantified with a LAS-3000 chemiluminescence image analyzer, and the numbers below the images indicate the mean $PrP^C$ expression relative to that in the parental N2a cells ($n$ = 2).

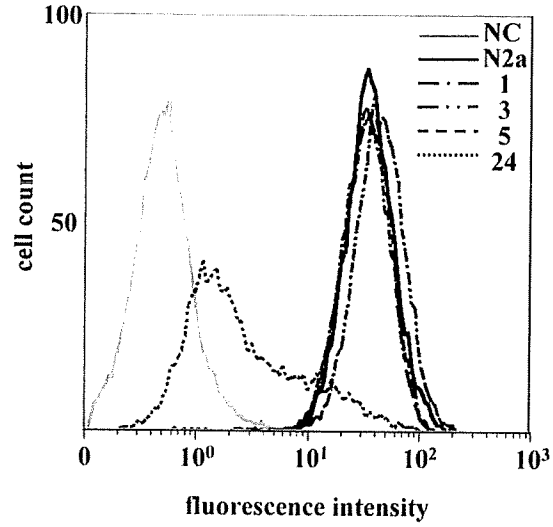


Fig. 3. Cell surface expression of $PrP^C$ in N2a subclones. $PrP^C$ on the cell surface of N2a and subclones N2a-1, -3, -5, and -24 was detected by flow cytometry. NC indicates the fluorescence intensity of N2a cells stained with negative control mAb P1-284 as a primary antibody. The $PrP^C$ expression levels relative to that in parental N2a cells were calculated from mean fluorescence intensities and are shown in Table 1.

Table 1. Levels of $PrP^C$ and PrP mRNA expression in N2a subclones

| N2a subclone | Relative to parental N2a cells | | |
|---|---|---|---|
| | Total $PrP^{C}$[a] | PrPC on cell surface[a] | PrP mRNA[a] |
| N2a-1 | 1.0 ± 0.7 | 1.1 ± 0.06 | 1.4 ± 0.4 |
| N2a-3 | 1.2 ± 0.5 | 1.3 ± 0.07 | 1.8 ± 0.7 |
| N2a-5 | 0.8 ± 0.2 | 1.0 ± 0.06 | 1.5 ± 0.4 |
| N2a-24 | 0.01 ± 0.004 | 0.07 ± 0.006 | 0.1 ± 0.04 |

[a]Means ± S.D. ($n$=3) relative to parental N2a cells.

-8, -19, -20, -23, and -24 in Fig. 1) were classified as unsusceptible because they were negative for $PrP^{Sc}$ at all passages examined. Subclones N2a-3 and -5, which showed intense $PrP^{Sc}$ bands at the ninth passage (Fig. 1), were positive for $PrP^{Sc}$ for more than 30 serial passages (data not shown). Thus, we used N2a-3 and -5 as representative prion-susceptible N2a subclones in the following experiments.

*Expression of $PrP^C$ and PrP Gene*

Because $PrP^C$ is essential for the propagation of prion and formation of $PrP^{Sc}$ (5–7), we first investigated $PrP^C$ expression in N2a subclones by WB (Fig. 2). As expected, prion-susceptible subclones expressed 0.4- to 2.6-fold as much $PrP^C$ as the parental N2a cells (Fig. 2). Among the prion-susceptible subclones, N2a-22 showed the lowest $PrP^C$ expression; it expressed only 0.4 ± 0.1-fold as much $PrP^C$ as the parental N2a cells. In contrast, $PrP^C$ expression varied among the prion-unsusceptible subclones. For instance, subclones N2a-1, -4, -8, -19, and -20 expressed similar level of $PrP^C$ as the parental N2a cells and susceptible subclones, whereas N2a-23 and -24 had lower $PrP^C$ expression than the parental cells, and actually, subclone N2a-24 expressed only one one-hundredth as much $PrP^C$ as the parental N2a cells.

Flow cytometric analysis showed that susceptible subclones N2a-3 and -5, and the unsusceptible subclone N2a-1 expressed $PrP^C$ on their cell surfaces, whereas, consistent with the WB analysis, the level of $PrP^C$ on the cell surface of the N2a-24 subclone was less than one-tenth of that in parental N2a cells (Fig. 3, Table 1). Furthermore, quantitative RT-PCR analysis also showed that the expression of the PrP gene in N2a-1, -3, and -5 was 1.4-, 1.8-, and 1.5-fold higher than in the parental N2a cells, respectively, whereas N2a-24 expressed only one-tenth as much PrP mRNA as the parental N2a cells (Table 1). Thus, the low level of $PrP^C$ expression in N2a-24 is probably due to inefficient transcription of the PrP gene. These results indicated that there are two types of prion-unsusceptible N2a subclones: one (e.g., N2a-1) that expresses a level of $PrP^C$ similar to prion-susceptible N2a cells, and another (e.g., N2a-24) that

expresses lower levels of $PrP^C$ than susceptible cells.

*Cellular Cholesterol Content of N2a Subclones*

The cellular cholesterol is reported to be important for the accumulation of $PrP^{Sc}$ in prion-infected N2a cells (2, 38). We therefore measured the cellular cholesterol content in representative N2a subclones; however, there was no significant difference in the cellular cholesterol contents between the parental N2a cells (8.3 ± 0.9 μg/mg protein), prion-unsusceptible subclones N2a-1 and -24 (8.6 ± 0.7 and 9.3 ± 0.9 μg/mg protein, respectively) and susceptible subclones N2a-3 and -5 (9.2 ± 0.4 and 7.9 ± 0.9 μg/mg protein, respectively).

*Binding of $PrP^{Sc}$ to N2a Subclones*

Binding of $PrP^{Sc}$ to the cells is considered to be the initial step in the prion infection after cells are inoculated with prion-infected brain homogenates. Thus, we examined the binding of $PrP^{Sc}$ to N2a subclones to investigate whether the binding step is involved in determining the prion-susceptibility and whether the expression of $PrP^C$ affects $PrP^{Sc}$ binding. Figure 4a shows the representative results for the binding of $PrP^{Sc}$ to N2a subclones at 37 C. $PrP^{Sc}$ bound equally to prion-susceptible (N2a-3 and -5) and unsusceptible N2a subclones (N2a-1 and -24). In addition, there was no significant difference in the amount of bound $PrP^{Sc}$ among N2a subclones and N2aII/9-4 that of stably overexpressed mouse $PrP^C$ (Fig. 5a). In addition, we observed a dose-dependent increase in $PrP^{Sc}$ binding both on ice and at 37 C, regardless of the prion susceptibility or level of $PrP^C$ in the cells (Fig. 4b). The increase of bound $PrP^{Sc}$ at 37 C suggests that a part of bound $PrP^{Sc}$ may be internalized during the incubation. These results revealed that prion susceptibility of these subclones is not determined by the binding and/or uptake of $PrP^{Sc}$ and that $PrP^C$ is not directly involved in the binding and/or uptake of $PrP^{Sc}$.

*Effect of Exogenously Introduced $PrP^C$ on Prion Susceptibility*

We speculated that the low level of $PrP^C$ expression in N2a-24 may explain its inability to support prion replication. To examine this possibility, we transfected N2a-1 and -24 cells with the mouse PrP gene expression vector pRc/EF-MoPrP and selected stable transformants in the presence of G418. We also used the $PrP^C$-overexpressing N2a subclone N2aII/9-4, which is a stable transformant by pRc/EF-MoPrP, as a control for G418-resistant prion-susceptible cells. Quantitative analysis of

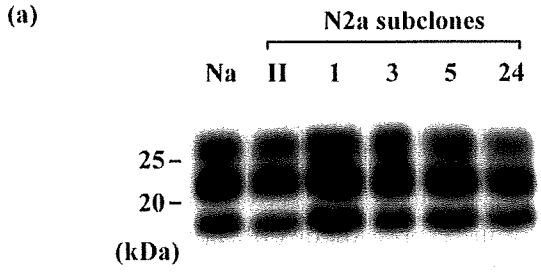


| N2a subclone | Relative to N2a (means ± S.D.) |
|---|---|
| N2aII/9-4 | 1.2 ± 0.5 |
| N2a-1 | 1.2 ± 0.2 |
| N2a-3 | 1.0 ± 0.3 |
| N2a-5 | 1.2 ± 0.4 |
| N2a-24 | 0.8 ± 0.2 |

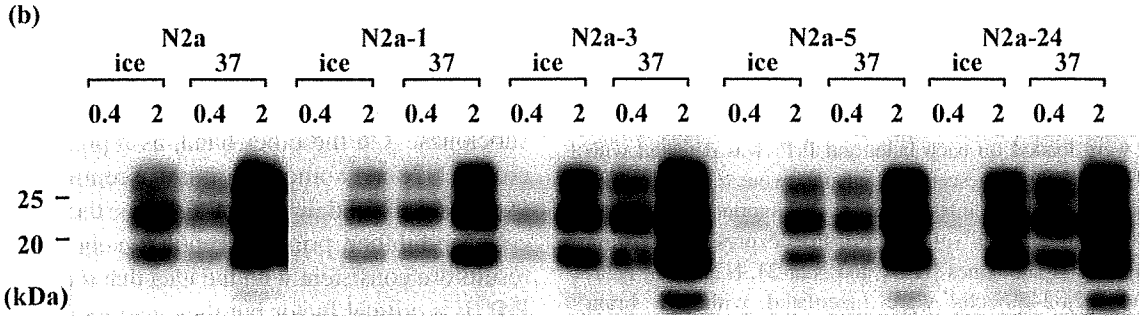


Fig. 4. Binding of $PrP^{Sc}$ to N2a subclones. (a) Representative results for the binding of $PrP^{Sc}$ to N2a cells. The cells were inoculated with 2% brain homogenate from mice infected with Chandler strain and then incubated at 37 C for 3 hr. Bound $PrP^{Sc}$ was detected as described in "Materials and Methods." The binding of $PrP^{Sc}$ relative to that in parental N2a cells is shown in the table on the right. Values in the table are the means ± S.D. from three independent experiments. Na, parental N2a cells; II, N2aII/9-4; 1, 3, 5, and 24, N2a subclone-1, -3, -5, and -24, respectively. (b) Dose- and temperature-dependent binding of $PrP^{Sc}$. The cells were inoculated with 0.4 and 2% brain homogenate from mice infected with Chandler strain and incubated at 37 C or on ice for 3 hr.

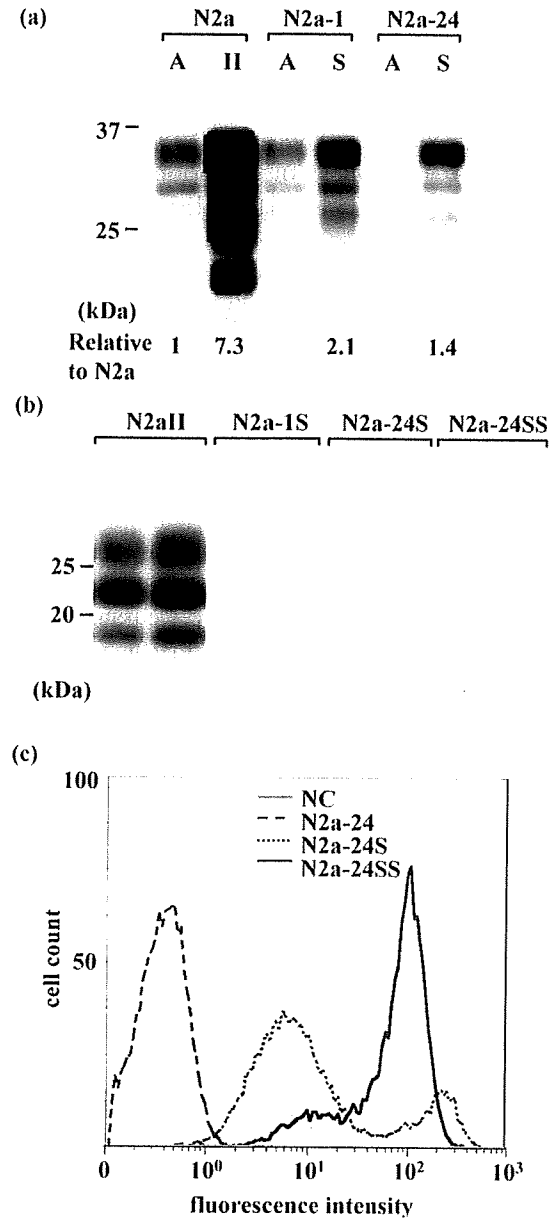


Fig. 5. (a) Expression of $PrP^C$ in N2a, N2a-1, and N2a-24 cells. N2a-1 and N2a-24 subclones were transfected with pRc/EF-MoPrP, and G418-resistant cells were selected. A indicates authentic cells, and S indicates G418-resistant cells. The G418-resistant N2a subclone II/9-4 was used as a control for G418-resistant prion-susceptible cells. Ten micrograms of the cell lysates were loaded on each lane, and $PrP^C$ was detected with mAb 31C6. The luminescence intensities were quantified, and the numbers below the image indicate the amount of $PrP^C$ relative to that in N2a cells. (b) Effect of $PrP^C$ expression on prion susceptibility of subclones N2a-1 and N2a-24. N2aII/9-4, N2a-1S, and N2a-24S cells were inoculated with 2% brain homogenate from mice infected with Chandler strain. $PrP^{Sc}$ was detected after the sixth consecutive passage. The results of duplicate samples are shown. (c) Cell surface expression of $PrP^C$ in N2a-24 cells. $PrP^C$ on the cell surface of N2a-24, 24S, and 24SS (selected by cell sorter) was detected by flow cytometry. NC indicates the fluorescence intensity of N2a-24S cells stained with negative control mAb P1-284 as a primary antibody.

WB revealed that the G418-resistant N2a-1 (N2a-1S) and N2a-24 (N2a-24S) cells expressed 2.1- and 1.4-fold more $PrP^C$ than the parental N2a cells (Fig. 5a). In addition, the G418-resistant N2a subclone N2aII/9-4 expressed 7.3-fold more $PrP^C$ than parental N2a cells. Flow cytometric analysis revealed that 39% of N2a-1S (data not shown) and 32% of N2a-24S cells expressed higher surface level of $PrP^C$ than the corresponding authentic subclones (Fig. 5c). These cells were inoculated with brain homogenate from prion-infected mice and then examined for $PrP^{Sc}$ after six serial passages. $PrP^{Sc}$ was detected in neither N2a-1S nor N2a-24S cells but was detected in N2aII/9-4 cells, suggesting that stable expression of $PrP^C$ did not confer the prion susceptibility to N2a-1 and N2a-24 cells (Fig. 5b). The fact that 32% of G418-resistant N2a-24S cells expressed elevated levels of $PrP^C$ might cause the inefficient prion replication in N2a-24S cells. To exclude this possibility, we collected $PrP^C$-overexpressing cells from G418-resistant N2a-24S cells by cell sorting. In this cell population (N2a-24SS), 79% of cells expressed elevated cell surface levels of $PrP^C$ (Fig. 5c); however, $PrP^{Sc}$ was not detected in these cells when they were inoculated with prion-infected brain homogenates (data not shown).

## Discussion

N2a cells have been reported to be composed of cells with different susceptibilities to prion infection (4, 9). One of the determinants of prion susceptibility is the expression of $PrP^C$ (3–5), but the quantitative relationship between $PrP^C$ expression and prion susceptibility is not well understood. We found considerable variation in the expression of $PrP^C$ in the N2a subclones established in this study. In particular, subclone N2a-24 expressed less than one one-hundredth as much $PrP^C$ as the parental N2a cells. Among the prion-susceptible N2a subclones, N2a-22 showed the lowest expression of $PrP^C$ but still expressed 0.4-fold as much $PrP^C$ as the parental N2a cells, suggesting that a substantial amount of $PrP^C$ is required to support prion propagation in N2a subclones. On the other hand, as represented by subclone N2a-1, some prion-unsusceptible subclones expressed similar levels of $PrP^C$ as the parental N2a cells and other prion-susceptible subclones. These results are consistent with the idea that the expression of $PrP^C$ is a critical factor but they also indicate that other factors and/or cellular microenvironments also determine the susceptibility of N2a cells to prion (4).

Exposing cells to prion-infected materials such as brain homogenates usually starts infection, and many cell lines can bind and internalize exogenous $PrP^{Sc}$ (24, 25, 39). Recently, Hijazi et al. showed that the similar

levels of $PrP^{Sc}$ bind to wild-type Chinese hamster ovary (CHO) cells, which do not express detectable levels of $PrP^C$, and CHO cells overexpressing $PrP^C$ (13). Magalhaes et al. also showed that uptake of exogenous $PrP^{Sc}$ does not require the presence of endogenous $PrP^C$ (25). In agreement with these observations, our results indicated that the binding of exogenous $PrP^{Sc}$ to the N2a cells was neither related to the prion susceptibility nor the level of $PrP^C$ expression. This also indicated that the binding of $PrP^{Sc}$ observed in this study did not account for the specific binding to $PrP^C$ but binding of $PrP^{Sc}$ to cell surface, although molecules and microenvironments involved in the binding are unclear. Cellular heparan sulfate (HS) has been reported to be involved in the uptake of exogenous $PrP^{Sc}$ following productive prion propagation in cells (14). In addition, the complex of LRP/LR and HS proteoglycan has been suggested to act as a receptor for $PrP^{Sc}$ (12, 15). We did not address the role of LRP/LR and HS proteoglycan in the binding of $PrP^{Sc}$ to N2a subclones; however, when the binding assay was carried out at 37 C, $PrP^{Sc}$ binding to the N2a subclones was increased regardless of the PrP expression level or prion susceptibility, suggesting that the uptake of $PrP^{Sc}$ may not be a major determinant of prion susceptibility in the N2a subclones. A recent report showed that the trafficking of exogenous $PrP^{Sc}$ in mouse septum neuron-derived SN56 cells differed according to the ability of prion to propagation in the cells (25). This suggested that prion susceptibility may be determined by events occurring after the uptake of $PrP^{Sc}$. Therefore it would be of interest to analyze the fate of $PrP^{Sc}$ after its binding to prion-susceptible and -unsusceptible N2a subclones.

In this study, we obtained a subclone, N2a-24, in which the expression of $PrP^C$ was much lower than in the parental N2a cells and other subclones. We confirmed that the low $PrP^C$ expression was due to inefficient expression of PrP mRNA. To address whether the low level of PrP gene expression is caused by genomic mutations in the regions involved in transcription of the PrP gene, we used long PCR to amplify the 5′- and 3′-flanking regions of exon 1 (nucleotides 6055–12058 in accession number U29186), which contain regions influencing PrP gene expression (17, 33) and carried out a direct sequencing of the amplified products. We did not find any nucleotide differences in this region between authentic N2a cells and subclones N2a-5 and N2a-24. We further analyzed the nucleotide sequences of exon 3 and its flanking regions (nucleotides 27096–30189 in accession number U29186), but again, the sequences were identical in authentic N2a cells and subclones N2a-5 and N2a-24 (data not shown). Thus, the low level of PrP gene expression in N2a-24 was not due to a mutation in the PrP gene but rather was probably due to a deficiency in the cellular machinery used for transcription of the PrP gene. In hepatic stellate cells, which express trace amounts of $PrP^C$, the expression of $PrP^C$ increased in response to $CCl_4$-induced hepatic damage (16). In addition, $PrP^C$ expression is increased in peripheral nerves during axon regeneration (28). These studies raised the possibility that the regulation of $PrP^C$ expression plays a role in neural and hepatic regeneration. In addition, PrP gene expression is developmentally regulated (26), but the molecular mechanism controlling PrP gene expression remains unclear. Thus, the low expression of the PrP gene in subclone N2a-24 despite a lack of mutations in the genomic region of the PrP gene, suggests that this subclone will be useful for analyzing the mechanism of PrP gene expression.

Host factors other than $PrP^C$ may be involved in the $PrP^{Sc}$ formation, i.e., prion replication, but little is known so far. A comparison of prion-susceptible and -resistant tissues could help to identify such host factors; however, large differences exist in gene expression profiles between tissues and thus comparison between tissues would complicate the identification of factors influencing prion susceptibility. A fine comparison would be possible, however, if the compared samples have similar biological properties. Hence, the N2a subclones established in this study should be useful for identifying host factors and cellular microenvironments influencing prion replication. Comprehensive comparison of these cells by transcriptomic and proteomic analyses will be useful in this regard and should help to elucidate the molecular mechanism of prion replication.

This work was supported by a grant from The 21st Century COE Program (A-1) and a Grant-in-Aid for Science Research (A) (grant 15208029) from the Ministry of Education, Culture, Sports, Science and Technology, Japan. This work was also supported by a grant from the Ministry of Health, Labour and Welfare, Japan.

## References

1) Applied Biosystems: User Bulletin #2 ABI Prism 7700 Sequence Detection System: December 11, 1997.
2) Bate, C., Salmona, M., Diomede, L., and Williams, A. 2004. Squalestatin cures prion-infected neurons and protects against prion neurotoxicity. J. Biol. Chem. **279**: 14983–14990.
3) Borchelt, D.R., Scott, M., Taraboulos, A., Stahl, N., and Prusiner, S.B. 1990. Scrapie and cellular prion proteins differ in their kinetics of synthesis and topology in cultured cells. J. Cell Biol. **110**: 743–752.
4) Bosque, P.J., and Prusiner, S.B. 2000. Cultured cell sublines highly susceptible to prion infection. J. Virol. **74**:

4377–4386.

5) Brandner, S., Raeber, A., Sailer, A., Blattler, T., Fischer, M., Weissmann, C., and Aguzzi, A. 1996. Normal host prion protein (PrPC) is required for scrapie spread within the central nervous system. Proc. Natl. Acad. Sci. U.S.A. **93**: 13148–13151.
6) Büeler, H., Aguzzi, A., Sailer, A., Greiner, R.A., Autenried, P., Aguet, M., and Weissmann, C. 1993. Mice devoid of PrP are resistant to scrapie. Cell **73**: 1339–1347.
7) Büeler, H., Fisher, M., Lang, Y., Bluethmann, H., Lipp, H.P., DeArmond, S.J., Prusiner, S.B., Aguet, M., and Weissmann, C. 1992. Normal development and behavior of mice lacking the neuronal cell-surface PrP protein. Nature **356**: 577–582.
8) Caughey, B., and Raymond, G.J. 1991. The scrapie-associated form of PrP is made from a cell surface precursor that is both protease- and phospholipase-sensitive. J. Biol. Chem. **266**: 18217–18223.
9) Enari, M., Flechsig, E., and Weissmann, C. 2001. Scrapie prion protein accumulation by scrapie-infected neuroblastoma cells abrogated by exposure to a prion protein antibody. Proc. Natl. Acad. Sci. U.S.A. **98**: 9295–9299.
10) Ertmer, A., Gilch, S., Yun, S.W., Flechsig, E., Klebl, B., Stein-Gerlach, M., Klein, M.A., and Schatzl, H.M. 2004. The tyrosine kinase inhibitor STI571 induces cellular clearance of PrP(Sc) in prion-infected cells. J. Biol. Chem. **279**: 41918–41927.
11) Fischer, M.B., Roeckl, C., Parizek, P., Schwarz, H.P., and Aguzzi, A. 2000. Binding of disease-associated prion protein to plasminogen. Nature **408**: 479–483.
12) Gauczynski, S., Nikles, D., El-Gogo, S., Papy-Garcia, D., Rey, C., Alban, S., Barritault, D., Lasmezas, C.I., and Weiss, S. 2006. The 37-kDa/67-kDa laminin receptor acts as a receptor for infectious prions and is inhibited by polysulfated glycanes. J. Infect. Dis. **194**: 702–709.
13) Hijazi, N., Kariv-Inbal, Z., Gasset, M., and Gabizon, R. 2005. PrPSc incorporation to cells requires endogenous glycosaminoglycan expression. J. Biol. Chem. **280**: 17057–17061.
14) Horonchik, L., Tzaban, S., Ben-Zaken, O., Yedidia, Y., Rouvinski, A., Papy-Garcia, D., Barritault, D., Vlodavsky, I., and Taraboulos, A. 2005. Heparan sulfate is a cellular receptor for purified infectious prions. J. Biol. Chem. **280**: 17062–17067.
15) Hundt, C., Peyrin, J.M., Haik, S., Gauczynski, S., Leucht, C., Rieger, R., Riley, M.L., Deslys, J.P., Dormont, D., Lasmezas, C.I., and Weiss, S. 2001. Identification of interaction domains of the prion protein with its 37-kDa/67-kDa laminin receptor. EMBO J. **20**: 5876–5886.
16) Ikeda, K., Kawada, N., Wang, Y.Q., Kadoya, H., Nakatani, K., Sato, M., and Kaneda, K. 1998. Expression of cellular prion protein in activated hepatic stellate cells. Am. J. Pathol. **153**: 1695–1700.
17) Inoue, S., Tanaka, M., Horiuchi, M., Ishiguro, N., and Shinagawa, M. 1997. Characterization of the bovine prion protein gene: the expression requires interaction between the promoter and intron. J. Vet. Med. Sci. **59**: 175–183.
18) Kaneko, K., Zulianello, L., Scott, M., Cooper, C.M., Wallace, A.C., James, T.L., Cohen, F.E., and Prusiner, S.B. 1997. Evidence for protein X binding to a discontinuous epitope on the cellular prion protein during scrapie prion propagation. Proc. Natl. Acad. Sci. U.S.A. **94**: 10069–10074.
19) Kim, C.L., Karino, A., Ishiguro, N., Shinagawa, M., Sato, M., and Horiuchi, M. 2004. Cell-surface retention of PrP(C) by anti-PrP antibody prevents protenase-resistant PrP formation. J. Gen. Virol. **85**: 3473–3482.
20) Kim, C.L., Umetani, A., Matui, T., Ishiguro, N., Shinagawa, M., and Horiuchi, M. 2004. Antigenic characterization of an abnormal isoform of prion protein using a new diverse panel of monoclonal antibodies. Virology **320**: 40–51.
21) Kurschner, C., and Morgan, J.I. 1995. The cellular prion protein (PrP) selectively binds to Bcl-2 in the yeast two-hybrid system. Brain Res. Mol. Brain Res. **30**: 165–168.
22) Leucht, C., Simoneau, S., Rey, C., Vana, K., Rieger, R., Lasmezas, C.I., and Weiss, S. 2003. The 37 kDa/67 kDa laminin receptor is required for PrP(Sc) propagation in scrapie-infected neuronal cells. EMBO Rep. **4**: 290–295.
23) Luhr, K.M., Nordstrom, E.K., Low, P., and Kristensson, K. 2004. Cathepsin B and L are involved in degradation of prions in GT1-1 neuronal cells. NeuroReport **15**: 1663–1667.
24) Luhr, K.M., Wallin, R.P., Ljunggren, H.G., Low, P., Taraboulos, A., and Kristensson, K. 2002. Processing and degradation of exogenous prion protein by CD11c(+) myeloid dendritic cells *in vitro*. J. Virol. **76**: 12259–12264.
25) Magalhaes, A.C., Baron, G.S., Lee, K.S., Steele-Mortimer, O., Dorward, D., Prado, M.A., and Caughey, B. 2005. Uptake and neuritic transport of scrapie prion protein coincident with infection of neuronal cells. J. Neurosci. **25**: 5207–5216.
26) Manson, J., West, J.D., Thomson, V., McBride, P., Kaufman, M.H., and Hope, J. 1992. The prion protein gene: a role in mouse embryogenesis? Development **115**: 117–122.
27) Mizushima, S., and Nagata, S. 1990. pEF-BOS, a powerful mammalian expression vector. Nucleic Acids Res. **18**: 5322.
28) Moya, K.L., Hassig, R., Breen, K.C., Volland, H., and Di Giamberardino, L. 2005. Axonal transport of the cellular prion protein is increased during axon regeneration. J. Neurochem. **92**: 1044–1053.
29) Naslavsky, N., Stein, R., Yanai, A., Friedlander, G., and Taraboulos, A. 1997. Characterization of detergent-insoluble complexes containing the cellular prion protein and its scrapie isoform. J. Biol. Chem. **272**: 6324–6331.
30) Nordstrom, E.K., Luhr, K.M., Ibanez, C., and Kristensson, K. 2005. Inhibitors of the mitogen-activated protein kinase kinase 1/2 signaling pathway clear prion-infected cells from PrPSc. J. Neurosci. **25**: 8451–8456.
31) Prusiner, S.B. 1991. Molecular biology of prion diseases. Science **252**: 1515–1522.
32) Rieger, R., Edenhofer, F., Lasmezas, C.I., and Weiss, S. 1997. The human 37-kDa laminin receptor precursor interacts with the prion protein in eukaryotic cells. Nat. Med. **3**: 1383–1388.
33) Saeki, K., Matsumoto, Y., Matsumoto, Y., and Onodera, T. 1996. Identification of a promoter region in the rat prion protein gene. Biochem. Biophys. Res. Commun. **219**:

47–52.
34) Salmona, M., Capobianco, R., Colombo, L., De Luigi, A., Rossi, G., Mangieri, M., Giaccone, G., Quaglio, E., Chiesa, R., Donati, M.B., Tagliavini, F., and Forloni, G. 2005. Role of plasminogen in propagation of scrapie. J. Virol. **79**: 11225–11230.
35) Schmitt-Ulms, G., Legname, G., Baldwin, M.A., Ball, H.L., Bradon, N., Bosque, P.J., Crossin, K.L., Edelman, G.M., DeArmond, S.J., Cohen, F.E., and Prusiner, S.B. 2001. Binding of neural cell adhesion molecules (N-CAMs) to the cellular prion protein. J. Mol. Biol. **314**: 1209–1225.
36) Stahl, N., Borchelt, D.R., and Prusiner, S.B. 1990. Differential release of cellular and scrapie prion proteins from cellular membranes by phosphatidylinositol-specific phospholipase C. Biochemistry **29**: 5405–5412.
37) Taraboulos, A., Raeber, A.J., Borchelt, D.R., Serban, D., and Prusiner, S.B. 1992. Synthesis and trafficking of prion proteins in cultured cells. Mol. Biol. Cell **3**: 851–863.
38) Taraboulos, A., Scott, M., Semenov, A., Avrahami, D., Laszlo, L., and Prusiner, S.B. 1995. Cholesterol depletion and modification of COOH-terminal targeting sequence of the prion protein inhibit formation of the scrapie isoform. J. Cell Biol. **129**: 121–132.
39) Taraboulos, A., Serban, D., and Prusiner, S.B. 1990. Scrapie prion proteins accumulate in the cytoplasm of persistently infected cultured cells. J. Cell Biol. **110**: 2117–2132.
40) Telling, G.C., Scott, M., Mastrianni, J., Gabizon, R., Torchia, M., Cohen, F.E., DeArmond, S.J., and Prusiner, S.B. 1995. Prion propagation in mice expressing human and chimeric PrP transgenes implicates the interaction of cellular PrP with another protein. Cell **83**: 79–90.
41) Vey, M., Pilkuhn, S., Wille, H., Nixon, R., DeArmond, S.J., Smart, E.J., Anderson, R.G., Taraboulos, A., and Prusiner, S.B. 1996. Subcellular colocalization of the cellular and scrapie prion proteins in caveolae-like membranous domains. Proc. Natl. Acad. Sci. U.S.A. **93**: 14945–14949.
42) Yadavalli, R., Guttmann, R.P., Seward, T., Centers, A.P., Williamson, R.A., and Telling, G.C. 2004. Calpain-dependent endoproteolytic cleavage of PrPSc modulates scrapie prion propagation. J. Biol. Chem. **279**: 21948–21956.

BMC Microbiology

BioMed Central

Research article

Open Access

# Heat shock cognate protein 70 contributes to *Brucella* invasion into trophoblast giant cells that cause infectious abortion

Kenta Watanabe[1,2], Masato Tachibana[1,2], Satoshi Tanaka[3], Hidefumi Furuoka[4], Motohiro Horiuchi[5], Hiroshi Suzuki[2,6] and Masahisa Watarai*[1]

Address: [1]Department of Veterinary Public Health, Faculty of Agriculture, Yamaguchi University, Yamaguchi, Japan, [2]Research Center for Protozoan Diseases, Obihiro University of Agriculture and Veterinary Medicine, Obihiro, Japan, [3]Department of Animal Resource Science and Veterinary Medical Science, the University of Tokyo, Tokyo, Japan, [4]Department of Veterinary Medical Science, Obihiro University of Agriculture and Veterinary Medicine, Obihiro, Japan, [5]Graduate School of Veterinary Medicine, Hokkaido University, Sapporo, Japan and [6]Department of Development and Medical Technology, the University of Tokyo, Tokyo, Japan

Email: Kenta Watanabe - s11042@st.obihiro.ac.jp; Masato Tachibana - s13028@st.obihiro.ac.jp; Satoshi Tanaka - asatoshi@mail.ecc.u-tokyo.ac.jp; Hidefumi Furuoka - furuoka@obihiro.ac.jp; Motohiro Horiuchi - horiuchi@vetmed.hokudai.ac.jp; Hiroshi Suzuki - hisuzuki@obihiro.ac.jp; Masahisa Watarai* - watarai@yamaguchi-u.ac.jp

* Corresponding author

Published: 5 December 2008

*BMC Microbiology* 2008, 8:212 doi:10.1186/1471-2180-8-212

Received: 21 April 2008
Accepted: 5 December 2008

This article is available from: http://www.biomedcentral.com/1471-2180/8/212



## Abstract

**Background:** The cell tropism of *Brucella abortus*, a causative agent of brucellosis and facultative intracellular pathogen, in the placenta is thought to be a key event of infectious abortion, although the molecular mechanism for this is largely unknown. There is a higher degree of bacterial colonization in the placenta than in other organs and many bacteria are detected in trophoblast giant (TG) cells in the placenta. In the present study, we investigated mechanism of *B. abortus* invasion into TG cells.

**Results:** We observed internalization and intracellular growth of *B. abortus* in cultured TG cells. A monoclonal antibody that inhibits bacterial internalization was isolated and this reacted with heat shock cognate protein 70 (Hsc70). Depletion and over expression of Hsc70 in TG cells inhibited and promoted bacterial internalization, respectively. IFN-γ receptor was expressed in TG cells and IFN-γ treatment enhanced the uptake of bacteria by TG cells. Administering the anti-Hsc70 antibody to pregnant mice served to prevent infectious abortion.

**Conclusion:** *B. abortus* infection of TG cells in placenta is mediated by Hsc70, and that such infection leads to infectious abortion.

## Background

Brucellosis is a widespread and economically important infectious disease of animals and humans caused by members of the genus *Brucella*. *Brucella* spp. are small gram-negative, facultative intracellular pathogens that cause abortion, retained placenta and infertility in numerous domestic and wild mammals, and a disease known as undulant fever in humans [1-3]. Transmission of *Brucella* spp. from infected animals to humans may be either direct or indirect. Direct transmission involves the respiratory, conjunctival and cutaneous routes, and is more important in people in close contact with infected animals. Indirect

transmission is through the consumption of contaminated dairy products [3]. *Brucella* spp. occasionally causes spontaneous abortion in pregnant women [4].

There have been several histological studies on the placentas of *Brucella* infected animals [5]. Further, it has been found that *Brucella* internalizes into the caprine erythrophagocytic trophoblastic epithelial cells from the maternal circulation [6] and that the internalized bacteria replicate within the rough endoplasmic reticulum, resulting in secondary infection of adjacent trophoblastic epithelial cells [6,7]. Researches have also shown that after necrosis of infected trophoblasts, large numbers of brucellae are released, and proximity of the fetal capillaries in the ulcerated placenta to the lumenal bacteria has been proposed as the source of the fetal bacteremia and further placental infection [6,8]. However, the molecular mechanism of abortion induced by *Brucella* spp. remains unknown.

The mouse model, particularly that using the unpregnant mouse, has been used extensively to study some aspects of the pathogenesis of brucellosis [2]. While brucellosis is known to primarily affect the reproductive tract in the natural host, little is known regarding the cellular and molecular mechanisms of *Brucella* infection in the pregnant mouse [9]. Although the structure of bovine placenta is completely different from mouse placenta, the infectious abortion model using the pregnant mouse is a powerful tool for investigating the mechanisms of *Brucella* pathogenesis. In our previous study, we demonstrated that *B. abortus* causes abortion in pregnant mice by inoculating bacteria on day 4.5 of gestation [10]. We found that there was a higher degree of bacterial colonization in the placenta than in other organs, that there were many bacteria in trophoblast giant (TG) cells in the placenta and that an intracellular replication-defective mutant did not induce abortion. These findings suggest that bacterial infection of TG cells plays a key role in abortion induced by *B. abortus* infection.

Pregnancy leads to a generalized suppression of the adaptive immune system, typified by significantly decreased cell-mediated immunity and reduced T helper cell (Th) 1 responsiveness [11-13]. This immunosuppressed state prevents maternal rejection of the fetus but has the unfortunate consequence of increasing maternal susceptibility to certain infectious agents [14,15]. Our previous study showed that a transient increase in interferon (IFN)-γ due to *Brucella* infection contributes to abortion in pregnant mice [10]. In addition to examining the balance of inflammatory and regulatory cytokines in bacteria infected pregnant mice, analysis of bacterial internalization into the TG cells, a specific host cells in placenta, will help to advance our knowledge regarding the control of *Brucella*-induced abortion.

In the present study, we investigated the internalization of *B. abortus* into TG cells and identified heat shock cognate protein 70 (Hsc70) as a candidate receptor against *Brucella* or bacterial uptake-associated molecule. We noted that IFN-γ enhances bacterial internalization into TG cells.

## Methods

### Bacterial strains

All *B. abortus* derivatives were from 544 (ATCC23448) smooth virulent *B. abortus* biovar 1 strains. GFP expressed 544 strain was used in this study [16,17]. *B. abortus* strains were maintained as frozen glycerol stocks and cultured on Brucella broth (Becton Dickinson) or Brucella broth containing 1.5% agar.

### Mice

Six to ten-week-old ICR female mice were individually mated to 6- to 10-week-old ICR male mice. The parent mice were obtained from CLEA Japan. Day 0.5 of gestation was the day the vaginal plug was observed. The normal gestational time for these mice is 19 days.

### Virulence in pregnant mice

Groups of five pregnant mice were infected intraperitoneally with approximately $10^4$ colony forming unit (CFU) of brucellae in 0.1 ml saline on day 4.5 of gestation [10]. On day 18.5 of gestation, placenta and spleen were removed and homogenized in phosphate buffered saline (PBS). Tissue homogenates were serially diluted with PBS and plated on Brucella agar to count the number of CFU in each organ. Fetuses were determined to be alive if there was a heartbeat, and dead if there was no heartbeat. The animal experiments were permitted by Animal Research Committee of Obihiro University of Agriculture and Veterinary Medicine.

### Cell culture

Trophoblast stem (TS) cells were cultured in TS medium in the presence of FGF4, heparin and mouse embryonic fibroblast (MEFs)-conditioned medium as described previously [18]. The TS medium was prepared by adding 20% fetal bovine serum (FBS), 1 mM sodium pyruvate, 100 μM β-mercaptoethanol, and 2 mM L-glutamine to RPMI 1640. To induce differentiation to trophoblast giant (TG) cells, the cells were cultured in the only TS medium alone for 3 days at 37°C in $CO_2$ incubator. The TG cells were seeded ($1-2 \times 10^5$ per well) in 48 well tissue culture plates for all assays.

### Efficiency of bacterial internalization and replication within cultured cells

Bacterial infection and intracellular survival assays were performed according to a modified version of the method of Kim *et al* [19]. *B. abortus* strains were deposited onto TS or TG cells at a multiplicity of infection (MOI) of 100 which had been grown on 48-well microtiter plates containing TS medium but no antibiotics by centrifugation at 150 × g for 10 min at room temperature. To measure bacterial internalization efficiency after 30 min of incubation at 37°C, the cells were washed once with TS medium and then incubated with TS medium containing gentamicin (30 μg/ml) for 30 min. Next, cells were washed three times with PBS and lysed with cold distilled water. CFU values were determined by serial dilution on Brucella plates. To measure intracellular replication efficiency, infected cells were incubated at 37°C for 30 min, washed once with TS medium and then incubated with TS medium containing gentamicin (30 μg/ml) for 2, 24, 48 and 72 h. The cell washing, lysis and plating procedures were the same as for the bacterial internalization efficiency assay. Percentage protection was determined by dividing the number of bacteria surviving by the number in the infectious inoculum. The purified the R2–25 antibody or recombinant IFN-γ (Cedarlane Laboratories) was added to the TS medium at the indicated concentrations 2 or 12 h before infection.

### F-actin staining

GFP-expressing bacteria were deposited onto the cultured cells by centrifugation and the incubation was conducted at 37°C for 30 min. The infected cells were incubated with TS medium containing gentamicin (30 μg/ml) at 37°C for 30 min to kill extracellular bacteria and were then fixed in 4% paraformaldehyde for 30 min at room temperature. Next, samples were permeabilized in 0.2% Triton X-100, washed three times with PBS and incubated with Alexa Fluor 594-phalloidin (Molecular Probes) at 20 μg/ml for 30 min at 37°C. After three washes with PBS, samples were placed in mounting medium (90% glycerol containing 1 mg/ml phenylenediamene in PBS, pH 9.0) and visualized by fluorescence microscopy.

### Isolation of monoclonal antibodies

Hybridomas producing monoclonal antibodies that inhibit bacterial internalization into TG cells were obtained from fusions of BALB/c P3-X63-Ag8.653 (8-azaguanine-resistant and non-producer cell line) myeloma cells with spleen cells from Wister rats that had been immunized with TG cells. The screening of hybridoma supernatants for inhibiting antibodies was performed by adding antibodies to the TS medium in a bacterial internalization assay. Monoclonal antibodies obtained from hybridoma supernatants were purified using a protein G column (GE Healthcare Life Science) and the class and subclass of the purified monoclonal antibodies were determined using an Immunogloblin Typing Kit (WAKO Pure Chemical). The R2–25 monoclonal antibody used in this study was typed as IgG1.

### Subcellular fractionation of TS and TG cells

TS and TG cells ($3 \times 10^5$/ml) were seeded into each well of a 6-well plate. Protein isolation for the cytoskeleton, nuclear, membrane, and cytosol fraction was performed using a ProteoExtract Subcellular Proteome Extraction Kit as described by the manufacturer (Calbiochem).

### Immunoblotting

The cell lysates (500 μg/ml) and fractionated proteins (50 μg/ml) were separated on 10% polyacrylamide gels and transferred to a PVDF membrane, which was incubated for 1 h at room temperature with primary antibody (0.5 μg/ml) in 5% skim milk. It was then washed three times in Tris buffered saline (TBS) with 0.02% Tween 20, incubated for 30 min with a horseradish peroxidase (HRP)-conjugated secondary antibody at 0.01 μg/ml and then washed again. Immunoreactions were visualized by ECL (GE Healthcare Life Science). Antibodies for β-actin, β-tublin and histone H1 were purchased from SIGMA or Abcam. Anti-IFN-γ receptor rabbit polyclonal antibody was purchased from Santa Cruz Biotechnology.

### Mass spectrometry analysis

Identification of proteins reacting with monoclonal antibodies that inhibited bacterial internalization into TG cells was conducted by means of nano LC-MS/MS analysis and a search of MASCOT database (APRO life Science Institute, Japan).

### RNA isolation and RT-PCR

The total RNA of TG cells was isolated using an RNA Purification Kit (Qiagen) and purified RNA samples were stored at -30°C until use. The RNA was quantified by absorption at 260 nm using a SmartSpec3000 spectrophotometer (Bio-Rad). RT-PCR was carried out using a Superscript II Kit (Invitrogen). The primers used for mouse Hsc70 or β-actin amplification had the following sequence 5'-GCAGCTGGGCCTACACACAAG-3' and 5'-CCCTGTGGAACAAAGCTACAC-3', or 5'-CGTGACATTAAGGAGAAGCTGTGC-3' and 5'-CTCAGGAGGAGCAATGATCTTGAT.

### Expression and purification of recombinant proteins

Mouse Hsc70 cDNA (GenBank Accession No. BC066191) was amplified from RNA isolated from TG cells by means of RT-PCR with the pair of primers described above. The product was cloned into the pCR2.1-TOPO vector (Invitrogen) (pCR-Hsc70). To achieve expression of recombinant Hsc70 protein, amplified DNA encoding Hsc70 from pCR-Hsc70 in PCR was cloned into pCold TF vector

(Takara Bio Inc.). The His-tagged Hsc70 was expressed in the *E. coli* strain DH5α, and its purification and cleavage of His-tagged by HRV 3C protease were performed as described by the manufacturer (Novagen). Bovine Hsc70 and the rat anti-Hsc70 monoclonal antibody (SPA-815) were obtained from Stressgen for use as control materials.

To achieve expression of Hsc70 in TG cells, amplified DNA encoding Hsc70 from pCR-Hsc70 in PCR was cloned into the pcDNA4/TO vector in the T-Rex System (Invitrogen). pcDNA4/TO-Hsc70 was transfected into TG cells using the FuGENE 6 Transfection Reagent (Roche) with a final concentration of 1.2 μg/ml.

#### *siRNA experiment*

The siRNA duplexes used for silencing mouse Hsc70 (target sequence: AACAAGTAACATGGAATAATA), and β-actin (target sequence: CACTGACTTGAGACCAATAAA) and AllStars Negative Control siRNA were purchased from QIGEN. TG cells were transiently transfected using oligofectamine (Invitrogen) with or without a final concentration of 10 nM for siRNAs.

#### *Immunofluorescence microscopy*

Samples grown on coverslips were washed twice with PBS, fixed with 4% paraformaldehyde in PBS for 30 min at room temperature, and permeabilized with or without 0.2% Triton X-100 in PBS for 20 min at room temperature. After blocking with 5% BSA in PBS, the cells were incubated with primary antibody (25 μg/ml) for 1 h at 37°C, and detection was conducted with TRITC-labeled goat anti-rat IgG (0.01 μg/ml) (Chemicon). Fluorescent images were taken using an Olympus BX51 microscope and a cooled CCD camera Olympus DP70.

#### In vivo *depletion of Hsc70*

Hsc70 was neutralized in the mice by administering an anti-mouse Hsc70 monoclonal antibody (clone R2-25)*in vivo* using 100 or 200 μg of antibody in a volume of 0.3 or 0.6 ml intraperitoneally 24 h before infection. Control mice were given 100 μg of normal rat IgG in a volume of 0.1 ml according to the same injection schedule as used for the anti-Hsc70 monoclonal antibody treated groups. Bacterial infection was conducted as described previously. On day 18.5 of gestation, fetuses were removed from the mice and a judgment made as to whether they were pregnant or not. Fetuses were determined to be alive if there was a heartbeat, and dead if there was no heartbeat.

#### *Statistical analysis*

All statistical analysis was conducted using the Student *t* test.

## Results

### B. abortus *internalizes and replicates in trophoblast giant cells*

We previously reported that there were many bacteria in trophoblast giant (TG) cells in the placenta by inoculation of pregnant mice with *B. abortus* [10]. To examine this bacterial infection into TG cells further, we used *in vitro* cell culture system of trophoblast stem (TS) cells and TG cells differentiated from TS cells. The *B. abortus* internalized into TG cells more efficiently than TS cells (Fig. 1A). We also investigated the intracellular replication of *B. abortus* in TS and TG cells. The bacteria replicated more efficiently in TG cells than TS cells (Fig. 1B).

Several intracellular pathogens attached to the host plasma membrane induce actin polymerization around the site of bacterial attachment and the process is essential for bacterial entry [20]. We therefore examined actin polymerization by means of fluorescence microscopy after 30 min and 48 h of incubation of TS and TG cells infected with *B. abortus*. It has been noted that differentiated TG cells dramatically rearrange their actin cytoskeleton into thick bundles of stress fibers [21]. There was no apparent actin polymerization around the site of the bacterial entry after 30 min incubation on TG cells or 48 h of incubation of infected TG cells (Fig. 1C).

#### *Isolation of monoclonal antibodies that inhibit bacterial internalization into TG cells*

To identify a receptor against *B. abortus* on TG cells, rats were immunized with TG cells, and monoclonal antibodies that inhibit bacterial internalization into TG cells were isolated. Seventy-five clones of bacterial internalization inhibiting antibodies (3.9%) were isolated from 1,920 hybridoma supernatants. From among the monoclonal antibodies, we selected R2-25, since it significantly inhibited internalization and showed clear reactions with protein in immunoblotting. The purified R2-25 antibody significantly inhibited bacterial internalization concentration dependently, but there was no inhibition with rat IgG (negative control) (Fig. 2A). The R2-25 antibody reacted with protein of around 70 kDa which was localized in membrane and cytosol, with the protein amount in the membrane fraction being especially large (Fig. 2C). On examining the distribution of protein reacting with R2-25 on the surface of TG cells by immunofluorescence microscopy, we observed an islet-like distribution on the surface of TG cells which was no permeabilized cells (Fig. 2B). It was difficult to detect the protein reacting with the R2-25 antibody on the surface of permeabilized cells.

#### *Antibody inhibiting bacterial internalization reacts with heat shock cognate protein 70*

We performed mass spectrometry analysis to identify the protein reacting with the R2-25 antibody. Proteins of the

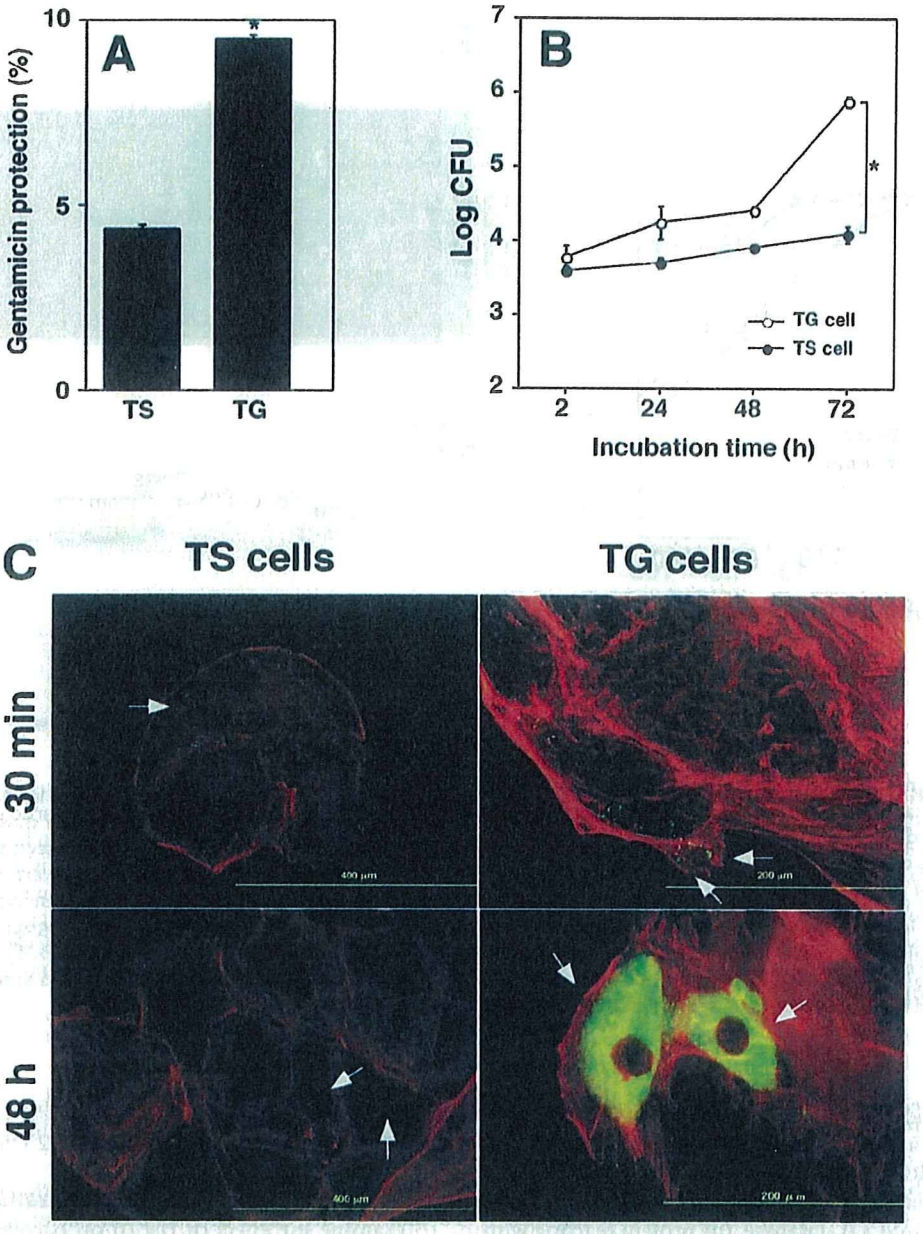


**Figure 1**

***B. abortus* infection in trophoblast giant cells.** (A) Bacterial internalization into trophoblast stem (TS) and giant (TG) cells. Data are the averages of triplicate samples from three identical experiments, and the error bars represent the standard deviations. Statistically significant difference between the bacterial internalization into TS and TG cells is indicated by asterisk (*, $P < 0.01$). (B) Intracellular replication of *B. abortus* in TS and TG cells. Datum points and error bars represent the mean of CFU of triplicate samples from a typical experiment (performed at least four times) and their standard deviations. Statistically significant difference between bacterial replication of *B. abortus* in TS and TG cells after 72 h of inoculation is indicated by asterisk (*, $P < 0.01$). (C) F-actin staining of bacteria infected cells. The figure shows GFP (bacteria) and Alexa Fluor 594 (actin filaments) channel merged images. Arrows indicate TS and TG cells containing bacteria.

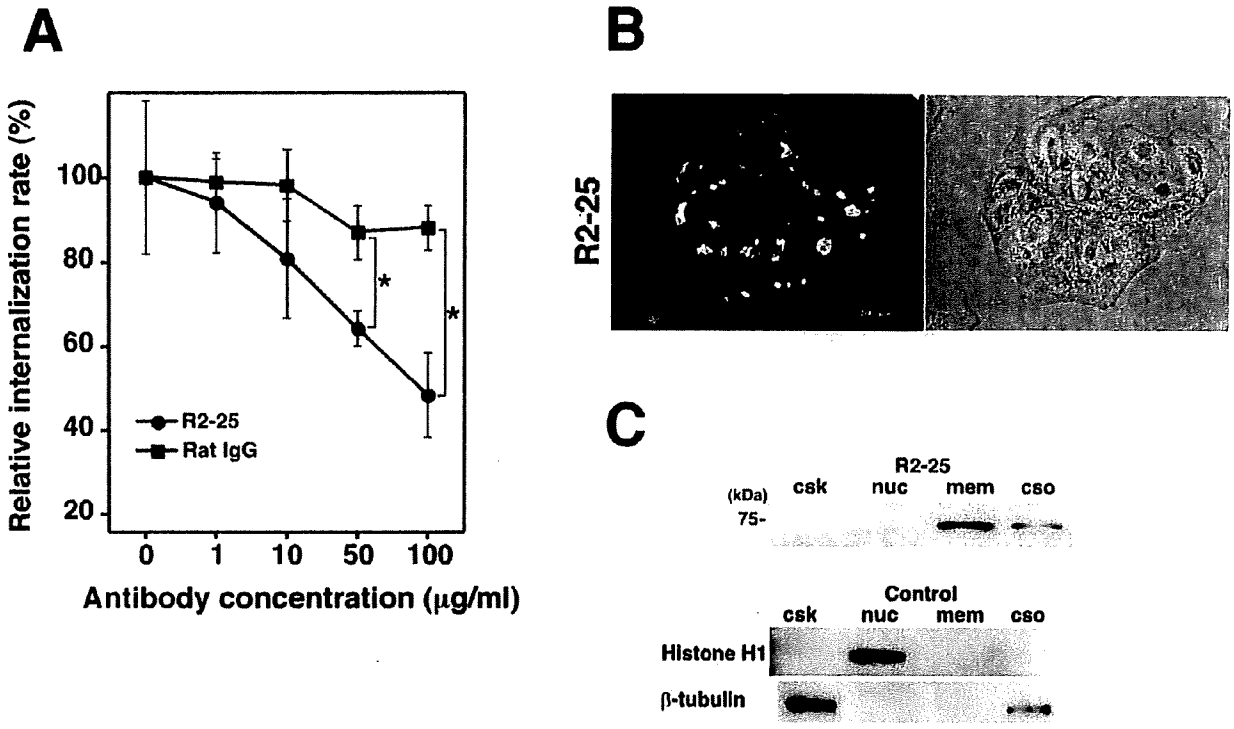


**Figure 2**

**Characterization of the monoclonal antibody that inhibits bacterial internalization into TG cells.** (A) Inhibition of bacterial internalization by the R2–25 antibody treatment. Data are the averages of triplicate samples from three identical experiments, and the error bars represent the standard deviations. Statistically significant differences between bacterial internalization into TG cells treated with the R2–25 antibody and those treated with rat IgG are indicated by asterisks (*, $P < 0.01$). (B) Distribution of protein reacting with monoclonal antibodies in TG cells. The left panels show fluorescence microscopy of the antibody stained TG cells and the right panels phase contrast microscopy of the corresponding microscopic fields. (C) Immunoblot analysis was performed on TG cell subcellular fractions with the monoclonal antibodies R2–25. Cells were fractionated to cytoskeleton (csk), nucleus (nuc), membrane (mem) and cytosol (cso). The anti-histone H1 and anti-β-tubulin antibody were used for fraction control for the nucleus and cytoskeleton.

membrane fraction were separated by SDS-PAGE and transferred to a PVDF membrane (Fig. 3A). The protein reacting with R2–25 was extracted from the PVDF membrane and the subjected to LC-MS/MS analysis. Through a search of the MASCOT database, the protein reacting with R2–25 was determined to be heat shock cognate protein 70 (Hsc70) (Fig. 3D). The anti-Hsc70 antibody also reacted with this protein (Fig. 3A). To confirm that the R2–25 antibody reacted with Hsc70, we tested its reactivity with mouse and bovine recombinant Hsc70. As expected, the R2–25 and anti-Hsc70 antibodies reacted with both types of recombinant Hsc70 (Fig. 3B and 3C). The mouse recombinant Hsc70 had a slightly greater molecular weight than the bovine recombinant Hsc70 because 25 amino acid residues had been added to the former after HRV 3C protease cleavage. These results indicate that the protein reacting with R2–25 was Hsc70.

***Hsc70 contributes to bacterial internalization into TG cells***

To examine the effect of Hsc70 on bacterial internalization into TG cells further, we reduced the amount of endogenous Hsc70 by transfecting Hsc70-specific small interfering RNA (siRNA) duplexes into the TG cells. After 48 h of transfection with Hsc70-specific siRNA, the expression level of Hsc70 was no longer detectable, but was not affected by transfection with β-actin or the control siRNA (Fig. 4A and 4D). Thus, the internalization efficiency of *B. abortus* into TG cells was significantly reduced by transfection with Hsc70-specific siRNA (Fig. 4C). Next, excessive production of endogenous Hsc70 was induced

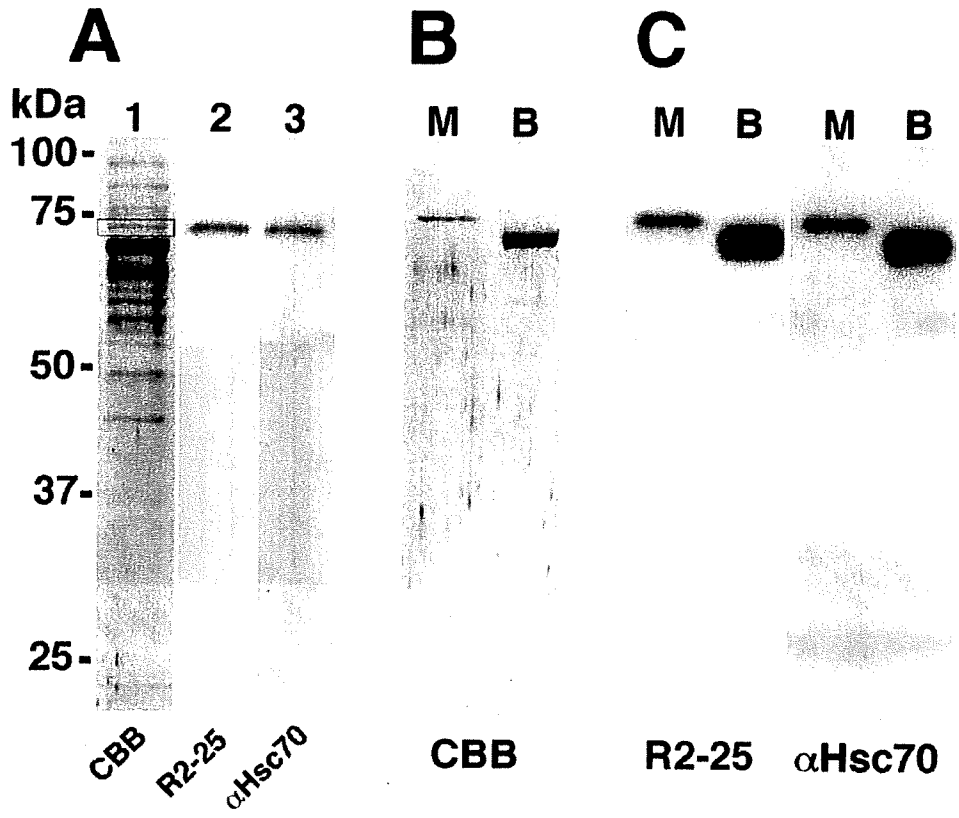


D

```
  1 MSKGPAVGID LGTTYSCVGV FQHGKVEIIA NDQGNRTTPS YVAFTDTERL
 51 IGDAAKNQVA MNPTNTVFDA KRLIGRRFDD AVVQSDMKHW PFMVVNDAGR
101 PKVQVEYKGE TKSFYPEEVS SMVLTKMKEI AEAYLGKTVT NAVVTVPAYF
151 NDSQRQATKD AGTIAGLNVL RIINEPTAAA IAYGLDKKVG AERNVLIFDL
201 GGGTFDVSIL TIEDGIFEVK STAGDTHLGG EDFDNRMVNH FIAEFKRKHK
251 KDISENKRAV RRLRTACERA KRTLSSSTQA SIEIDSLYEG IDFYTSITRA
301 RFEELNADLF RGTLDPVEKA LRDAKLDKSQ IHDIVLVGGS TRIPKIQKLL
351 QDFFNGKELN KSINPDEAVA YGAAVQAAIL SGDKSENVQD LLLLDVTPLS
401 LGIETAGGVM TVLIKRNTTI PTKQTQTFTT YSDNQPGVLI QVYEGERAMT
451 KDNNLLGKFE LTGIPPAPRG VPQIEVTFDI DANGILNVSA VDKSTGKENK
501 ITITNDKGRL SKEDIERMVQ EAEKYKAEDE KQRDKVSSKN SLESYAFNMK
551 ATVEDEKLQG KINDEDKQKI LDKCNEIISW LDKNQTAEEE EFEHQQKELE
601 KVCNPIITKL YQSAGGMPGG MPGGFPGGGA PPSGGASSGP TIEEVD
```

**Figure 3**

**Bacterial internalization inhibiting antibodies react with Hsc70.** (A) A membrane to which TG cell membrane fraction proteins had been transferred was stained with Coomassie brilliant blue (CBB) (lane 1), immunoblotted with the R2–25 antibody (lane 2) and the anti-Hsc70 antibody (clone SPA-815) (lane 3). (B) CBB staining of membrane to which mouse (M) or bovine (B) recombinant Hsc70 had been transferred. (C) Immunoblot analysis of mouse (M) or bovine (B) recombinant Hsc70 with R2–25 antibody and anti-Hsc70 antibody (clone SPA-815). (D) Amino acid sequences of Hsc70. The protein reacting with R2–25 was extracted from the PVDF membrane (square in lane 1 of panel A) and was used for LC-MS/MS analysis. The amino acids detected for Hsc70 in the analysis are shown in bold.